Master Thesis in Geographical Information Science nr 165

Geographic polarization and clustering of partisan voting: A local-level analysis of Stockholm Municipality

2023

Department of

Physical Geography and Ecosystem Science

Centre for Geographical Information Systems

Lund University
Sölvegatan 12

Jonas Almén (2023). Geographic polarization and clustering of partisan voting: A local-level analysis of Stockholm Municipality

Master degree thesis, 30/ credits in Master in Geographical Information Science
Department of Physical Geography and Ecosystem Science, Lund University

Abstract

In the last decade, the topic of political polarization has become a growing concern within academic and public debate. Many highlight the linkage between increased political polarization and democratic problems such as political tribalism and uncivil activism. It is also argued to be a global phenomenon. Despite this, research on political polarization - and its outcome in space (i.e. geographic polarization) - has predominately been conducted in the United States where an increased tendency for the partisan vote to spatially cluster at the local-most level of neighborhoods has been observed. However, this also means that no studies have been conducted in political systems that is not characterized by the binary two-party-system.

This study investigates the prevalence of geographic polarization within the Municipality of Stockholm, Sweden between 1998 and 2018. As the topic of geographic polarization has been largely neglected in Sweden, the aim of this study is to gain insight on the prevalence, magnitude and longitudinal development of polarization in the Swedish multi-party system context.

The methodological approach of this study is to measure the degree of geographical polarization, at electoral districts, utilizing Global and Local Moran's I, a common spatial regression statistic within geographic information systems (GIS) which has been used in several studies to examine the degree in which the partisan vote tends to cluster. This is done at [1] the Global level, i.e. the overall tendency for the partisan vote to cluster, and [2] the Local level, the tendency for the partisan vote to cluster at different magnitudes across neighborhoods within the municipality.

As results show, within the Municipality of Stockholm there was a decreasing trend of clustering of the partisan vote between the elections of 1998 and 2010. Between 2010 and 2018 there was an increasing trend of the partisan vote to cluster. This is a much more ambiguous result compared to similar studies in the United States, where similar studies show a much clearer linear trend. At the local level, the magnitude in which the partisan vote tend to cluster at different parts of the city is clear. The right-wing vote is mostly clustered at the central part of the city, mainly around the neighborhoods of Norrmalm and Östermalm. The left-wing vote is mostly clustered in the Sub-urbs of Rinkeby-Kista and Spånga-Tensta. This pattern is repeated for all elections.

In conclusion, between 1998 and 2018, the Municipality of Stockholm showed a varying degree of geographic polarization, but no unambiguous evidence of an increase. The municipality was just as geographically polarized as 2018 as of 1998. At the local level, the tendency for the partisan vote to cluster at different parts of the municipality is repeated at each election, indicating a stable electoral geography. Hence, claims of an increased geographic polarization within the municipality cannot be supported.

Keywords: Geography, GIS, Spatial Analysis, Spatial Autocorrelation, MAUP, Electoral Geography, Political Polarization, Geographic Polarization, Stockholm Municipality.

Table of Contents

List of Tables

List of Figures

List of Abbreviations

GIS	Geographic Information Systems
MAUP	Modifiable Areal Unit Problem
BSH	Big Sort Hypothesis
SCB	Statistics Sweden (swe: Statistiska centralbyrån)

1. Introduction

In the light of the political and social turmoil of the recent decade, the public and academic debate on political polarization has received increased attention. Political polarization is considered a global phenomenon by some (Carothers & O'Donohue, 2019), and the later U.S. elections and the British referendum on Brexit are often held as prime examples. An increasing amount of literature seeks to examine the prevalence and magnitude of, and driving forces behind, political polarization, often with the U.S. as the main focus (Levendusky, 2009; Böttcher & Gersbach, 2020). Societal impacts of political polarization include partisan and political bias, uncivil activism and negative affective emotions towards "the others" (Mason, 2015; Shanto, et al., 2019)

Evidence of political polarization is often studied by examining the opinions of important societal actors such as the electorate (voters), political parties, political representatives and media outlets (Oscarsson, et al., 2021). However, an often-neglected aspect of political polarization is its manifestation in space through the electoral geography. In the United States, the topic of *geographic polarization,* has received increasing attention by the apparent "blue state vs red state" division and the debate around the "Big Sort Hypothesis," which suggests that American residents are increasingly geographically clustered in segregated neighborhoods together with people of "like-minded" political beliefs and voting behavior (Bishop, 2009).

Following the debate sparked by Bishop (2009), a growing number of studies in the United States conclude a prevalent and increased geographical polarization. Most commonly, this is done by utilizing methodologies from spatial analysis and GIS together with thematic map visualizations. Evidence has been found at different scales between the rural and urban (Scala & Johnson, 2017) census divisions, states and counties (Johnston, et al., 2016) and more strikingly, at the local level of electoral districts and neighborhoods (Sussell, 2013; Myers, 2013; Kinsella,et al., 2015; Ryne Rohlaa, et al., 2018; Kinsella, et al., 2021). These local micro-level studies conclude that analysis based on aggregated geographical entities, such as states and counties, mask the prevalence of local polarization due to the ecological fallacy, meaning that conclusions on sub-entities are drawn from aggregate data and may therefore not be valid (Li, et al., 2018). Consequently, the "Big Sort Hypothesis" has gained increasing support by local-level analysis, further adding to the idea of a politically and geographically polarized nation.

Compared to the United States, the topic of geographic polarization has gained very little scientific attention in Sweden. This is despite the fact that public discourse on political polarization has been lively during recent elections (Knutson, 2019; Von Arnold, 2021). A recent report on the topic of political polarization in Sweden concludes that a slight increase in affective polarization (dislike for those with another political affiliation) amongst the electorate has occurred, but not to the extent it has developed in the United Sates (Oscarsson, et al., 2021). However, the report does not examine the geographic polarization of the electorate. This despite that the partisan vote of the Swedish electorate is not equally distributed in space. For instance, at the regional level, municipalities in northern Sweden attracts more left-wing votes than southern Sweden (Michaud et.al., 2021). At the local and intra-urban level of inner-city Stockholm (the country's capital), the tendency for the neighborhoods to the north to vote right, and to the south to vote left, is a widespread assumption to many people. Despite these known voting patterns, the degree to which they are clustered in space has never been examined. Hence, historic or present geographic polarization in a Swedish context remains unstudied, and questions regarding its prevalence, spatial extent, degree, and variation at recent elections are unknown.

1.2 Aim and research questions.

The aim of this study is to examine the spatial and temporal variation of geographic polarization within the electorate of the municipality of Stockholm, the country's capital and largest urban area. Methodologically, this is done through statistical testing by Global and Local Moran's I at the local scale of electoral districts. Temporally, six election results are analyzed over a twenty-year period (between 1998 and 2018). The outcome of this analysis is presented in the form of thematic maps, as well as a timeline on the degree of polarization at each election. The main research questions are:

1. **How has the degree of geographic polarization varied for each election?**
2. **How has the local degree of geographic polarization varied across the municipality, for each election?**

2. Background and Key Topics

2.1 Electoral Geography

Electoral geography is the study of the interaction between space, place and the electoral process (Pattie & Johnston, 2009; Storey, 2009). As a sub-field of Political Geography, two of the main concerns within Electoral Geography are: 1) analysis of demographic and locally derived effects on voting behavior, and 2) the spatial structure of election results, i.e. geographic *voting patterns*.

The topic on the effects on voting behavior is linked to the broader debate within Human Geography regarding *compositional* and *contextual* effects and their possible complex interactions (Pattie & Johnston, 2009). Compositional effects on voting behavior are the result of the demographic structure (e.g. class, gender and education) and their different voting tendencies. In contrast to this, contextual effects are factors deriving from the direct spatial environment in which the electorate encounters, e.g. place-specific campaigning and local economic and social circumstances (Johnston et al., 2004; Cutts & Webber, 2010).

Studies that focus on the voting patterns of election results have historically been an integral topic of electoral geography. Despite their lack of ability to explain why voting behavior differs across space, it still has a strong following, especially in the United States (Forest, 2017; Pattie & Johnston, 2009). Studies on voting patterns are predominately conducted on aggregated geographical data, mainly because of it's availability and extensive geographical coverage.

Due to being limited to aggregate geographical data, studies on voting patterns are subject to the Modifiable Areal Unit Problem (MAUP) and potentially the ecological fallacy (Pattie & Johnston, 2009). MAUP is a term for the statistical bias inflicted by the variability and inconsistency that is unavoidably inherited in aggregated geographical data. The problem of MAUP consists of two sub-problems related to: (a) scale and (b) zoning (Wong, 2009). The problem of scale is due to the fact that different results may occur when representing data at different hierarchical scale-levels e.g. counties, states and divisions. As an example, the representation of an election result within a state may be presented differently depending on if data is presented at the scale of neighborhoods or counties. Also, the problem of scale is related to the concept of ecological fallacy which occurs when conclusions on individual sub-entities are drawn from coarser aggregate data (Li, et al., 2018). The problem of zoning is due to the effect that different groupings of smaller areal units, or drawing of their boundaries, have on the apparent result. As an example, the election result of an electoral district could radically change just by redrawing its borders. Theoretically, there are endless varying ways to group geographical units, but also endless ways in which its borders can be drawn, making the analytical result statistically affected by the arbitrary geographic delineation of the data.

2.2 Political Polarization

Polarization as a concept has been widely used and studied within political science. Within these studies the term political polarization is often used to explain the relationship between discourses of political opinions, values and behaviors for a political issue (Oscarsson, et al., 2021). In a democracy, carriers of these discourses include important societal actors such as political parties, elected officials, the media and the voting electorate.

Conceptually, polarization (political or otherwise) can be viewed as both a process and a state (DiMaggio, et al., 1998). Polarization as a state refers to the measured level, in relation to a theoretical maximum, in which the opinions on a topic are opposed. Polarization as a process refers to the measured increase of these opposing opinions through time. As argued by Fiorina & Abrams (2008), when measured through the conceptualization of a state, polarization is often a matter of judgement as it can be argued to exist at the tail of any distribution, at any given time. Therefore, any robust analysis of polarization should be conceptualized as a process with measurable levels of polarization across time to uncover any trends on increase, decrease or stability.

The process of polarization is often defined by an increase in *extremism*, *divergence,* or *sorting* between actors along the political dimension (Oscarsson, et al., 2021). In a process of increased extremism, the distribution of actors is increased at the polar opposites of the political spectrum and decreased in the middle. An increase in divergence describes when the whole constellation of actors increases their relative distance towards each other. Polarization by sorting is where there is no movement along the political dimension but the *distinction* of each position in the political dimension is increased.

Polarization as a sorting process is often emphasized within the political debate of the United States. In the American context, it is argued that the process of increased sorting of elite actors within the Democratic and Republican party has also influenced the electorate as regards to their party preference (*partisan sorting*) (Levendusky, 2009: Oscarsson et al., 2021). Through this sorting process, the partisan preference of the electorate not only becomes more aligned by political ideology but also with other social and cultural divisions such as education, ethnicity, religiosity and *geographical location of residence*. In other words, the distinction of what constitute a “true” Republican or Democrat is increased. It is argued that this process has societal impacts up to a point where a “tribalization” along more and more homogenized groups are evident (Oscarsson, et al., 2021), with increased political bias, uncivil activism and dislike towards “the other” as a consequence (Mason, 2015; Shanto et al., 2019).

In comparison with the United States, fewer studies on Political Polarization have been conducted in a Swedish political context. In a report by Oscarsson, et al., (2021) the topic of political polarization within the Swedish electorate is investigated by analyzing several longitudinal data sets on party preference and social, economic and cultural affiliation of the electorate such as class, education and urban or rural residence. The report concludes that generally, partisan sorting by social group affiliation shows no sign of increase in Sweden, in stark contrast to the situation in the United States.

2.3 Geographic Polarization

Studies on *geographic* polarization seek to examine the location, extent, and magnitude of political polarization in space (Kinsella C. , McTague, Raleigh, & a, 2015). The public and scientific debate on geographical polarization is noted by Bishop (2009) who argues that the partisan sorting in the United States also has profound influence on the political geography due to the sorting process of migration at regional, state and community levels i.e. *geographic sorting*. As a consequence of this sorting process, it is argued that more and more Americans tend to cluster locally in politically segregated neighborhoods with like-minded values and voting behaviors. While the initial empirical support for the “Big Sort Hypothesis” (BSH) presented by Bishop (2009) has been questioned due to arbitrary temporal election comparisons (Abrams & Fiorina, 2012), the hypothesis of an increased geographic polarization has sparked a substantial amount of debate and scientific literature on the topic.

2.3.1 Geographic Context of Previous Studies

Scientific research on geographic polarization has received very little notice outside the societal and political context of United States despite the argument that *political* polarization is a global phenomenon (Carothers & O’Donohue, 2019). However, a few studies have been conducted in Europe prior to the last decades debate on polarization, such as the case of intra-urban polarization in Moscow (O'Loughlin, et al., 1997) and city-suburban voting polarization in the United Kingdom (Walks, 2005).

As recent studies have had a predominant focus on the United States, most studies have been conducted at single or multiple scales within the American political geography. These include divisions, states, counties and various smaller geographical entities. In single-scale studies, counties have traditionally been the most frequent choice, both within studies on geographic polarization and electoral geography in general, due to: (1) the high degree of availability and accessibility of geographical data, (2) the fact that the local-most scales are where the political boundaries are intact through time, and (3) the existence of aggregate economic and social data local at these scales which allow for analysis of compositional effects (Kinsella C. et al., 2021). In fact, initial support for the BSH was underpinned by county-level data (Bishop, 2009), as was a critical rejection of that hypothesis by Abrams & Fiorina (2012). Further on, county-level studies have been conducted to uncover the geography of polarization by geographical change in party alignment and regional and intra-regional differences (McKee & Teigen, 2009; Morrill & Webster, 2015). Other studies have examined the process of polarization through longer time-series and found support of an increased geographical polarization (Morrill, Knopp, & Brown, 2011; Lang & Pearson-Merkowitz, 2015; Johnston, et al., 2020). In contrast to these findings, long-term historical research highlights the overall stability of geographical polarization within the American counties (Darmofal & Strickler, 2019). As put forward by Darmofal & Strickler (2019), through the time period of 1828-2016, counties within the United States have shown a varying degree of geographical polarization. The highest degrees of polarization were found around the mid-twentieth century, with recent elections more akin to degrees of the nineteenth-century, indicating that the county is not more polarized today as of the last century.

Studies on multiple scales often utilize multi-level-modeling to analyze polarization at several scales. Johnston, et al., (2016) examined geographical polarization of the presidential vote between 1992 and 2012 which was found to have increased at all scales examined (division, state, and county). Similarly, Sussell (2013) found evidence for increased segregation amongst Republicans and Democrats in the State of California, between 1992 and 2010, at the level of counties, block groups and census tracts (a sub-entity of a county). In a study by Ryne Rohlaa et al. (2018) the degree of polarization was measured not only on division, states and county but also at the local-most geographical entity of electoral districts, where the polarization was found to be significantly higher than at coarser scales.

2.3.2 Local Level Analysis

Compared to county-level studies, fewer studies have been conducted at the local scale such as electoral districts. In relation to findings by Ryne Rohlaa et al. (2018) where polarization at this scale was found most significant, geographic polarization is surprisingly understudied at this level despite that fact that they operate at the local level of ”neighborhoods” and ”streets” in which the geographical sorting as hypothesized by Bishop (2009) is supposed to occur. However, the need of local analysis at this level has been addressed in many studies (Sussell, 2013; Johnston et al., 2016; Ryne Rohlaa et al., 2018; Johnston, et al., 2020), but because a lack of availability, accessibility and methodological problems related to their frequent boundary-redrawing, only a few studies have been conducted.

Despite being few in number, local level studies have produced insightful evidence of local geographical polarization by utilizing spatial regression-techniques common within GIS to localize “hot-spots” and patterns of clustering. In a case study covering the extent of Texas, Myers (2013) found evidence that the change in the Republican vote amongst local electoral districts became significantly and increasingly clustered between the election years of 1996-2010. Clusters of the higher-than-average increase of the Republican vote were generally located in rural areas, while lower-then-average clusters were found in the metropolitan areas of Dallas, Houston and Austin. Examining the greater metropolitan area of Cincinnati, findings by Kinsella C. et al., (2015) also indicated that the partisan vote is significantly spatially clustered, and the degree of clustering had increased within the area between the elections of 1976 and 2008. Similar to Myers (2013), a pattern of an increasingly Republican rural, and a Democratic urban geography was proposed. In addition to localizing clusters of like-minded voting, the local analysis by Kinsella C. et al., (2015) also detected diverging electoral districts where this overall global pattern did not apply (e.g. predominantly Republican electoral districts in an otherwise Democratic area).

Important conclusions from these local-analysis are the evident “unmasking” effect they have on macro-geographical units (e.g. counties), uncovering their potential ecological fallacy. This topic of is explicitly covered by Kinsella C. et al., (2021) by exploring local geographic polarization at the 10 most “purple counties” (a term for counties with even turnout for the republican and democrat vote). In county-level studies, occurrence of these is often held as valid examples of “non-polarization” and contrasted to “land-slide-counties” due to their even turnout (Bishop, 2009; Abrams & Fiorina, 2012; Johnston et al, 2020). However, when examined at the local level of electoral districts, these counties show great internal polarization due to geographical clustering at different parts within them, showcasing the importance of local analysis in examining geographical polarization.

2.5 The electoral system of Sweden

The Swedish election system is a multi-party parliamentary democracy based on universal suffrage with a proportional representation (Valmyndigheten, 2021a). Elections are held at three different assemblies at three different geographical scales that include the *parliamentary, the county* and the *municipality.* As the election system is proportional, the number of seats for each general assembly is to a great extent in direct proportion to the percentage share for each party. To gain representation in the parliament, a political party must reach 4% of the total vote. The proportional representation can be contrasted to the election systems more common in the anglosphere (such as United States and United Kingdom) where plurality voting is premiered, meaning that the candidate, or political party, who gains the most votes get to represent the district subject to the election process. Also, the multi-party system can be contrasted with the Two-Party-system in United States which in modern times have been dominated by the Republican and Democrat parties.

The geographical administration of Swedish elections is governed by The Elections Act (SFS 2005:837). By this law the country should be divided into constituencies (swe: *Valkretsar*) that ensures geographical representation at each assembly level for each election. To deal with the administration of the electoral process, each municipality should be divided into several *valdistrikt* (electoral districts), all providing one polling station. These electoral districts are the local-most geographical entity in the electoral geography. As stated in the The Elections Act (SFS 2005:837), each electoral district should incorporate between 1 000 and 2 000 entitled voters, and in exceptional cases where this criterion can’t be met it has to be approved by the County Administrative Board governing that municipality. Naturally, as municipalities undergo demographic changes at different localities within its area, the geography of the electoral districts are redrawn to correspond with the population size for each election.

3 Study Area

Stockholm municipality is the capital and largest city in Sweden with a population > 960 000 inhabitants as of 2021. Due to its size and general cultural influence on Sweden, the municipality is a natural choice for a first ever case study on local geographic polarization in Sweden. The municipality of Stockholm consists of 21 529 ha of land area (see Table 1) and is distributed across both the Swedish Mainland and several smaller islands which constitute much of the central city. Because of this, the biophysical environment of the city is heavily characterized by water which separates many of the city's neighborhoods. Population-wise, the city is characterized by a generally affluent city center with relatively poorer neighborhoods situated at its sub-urban periphery. For maps on population, mean income and voting percentage per neighborhood district, see Figure 1, 2 and 3.

Table 1. Administrative districts with geographical statistics as of election year of 2018. Note that the statistics of Södermalm also incorporate Hammarby Sjöstad (Stockholms Stad, 2019; Stockholms Stad, 2020; Stockholms Stad, 2021a).

Municipal District	Neighborhood District	Land Area (ha)	Population	Mean Income (SEK/year), age 20-64)	Voting percentage	Electoral Districts
Innerstan	Kungsholmen	485	71 191	497 100	85.9	45
	Norrmalm	492	71 800	535 100	85.7	44
	Östermalm	1800	76 587	544 200	84.3	47
	Södermalm	800	130 034	444 600	86.6	71
Västerort	Bromma	2460	80 045	496 100	85.4	51
	Hässelby-Vällingby	1960	75 904	354 600	74.7	43
	Rinkeby-Kista	1179	50 404	273 600	56.4	21
	Spånga-Tensta	1285	39 106	345 700	70.1	21
Söderort	Enskede-Årsta-Vantör	2114	100 859	366 400	78.4	59
	Farsta	1544	33 742	347 300	78.2	35
	Hägersten-Älvsjö	1308	90 203	366 400	84.6	70
	Hammarby Sjöstad	125	18 902	505 800	89.7	11
	Skärholmen	886	37 349	277 300	63.6	22
	Skarpnäck	1550	46 427	368 500	82.7	27
	Whole Municipality	21 592	949 671	420 700	83.5	573

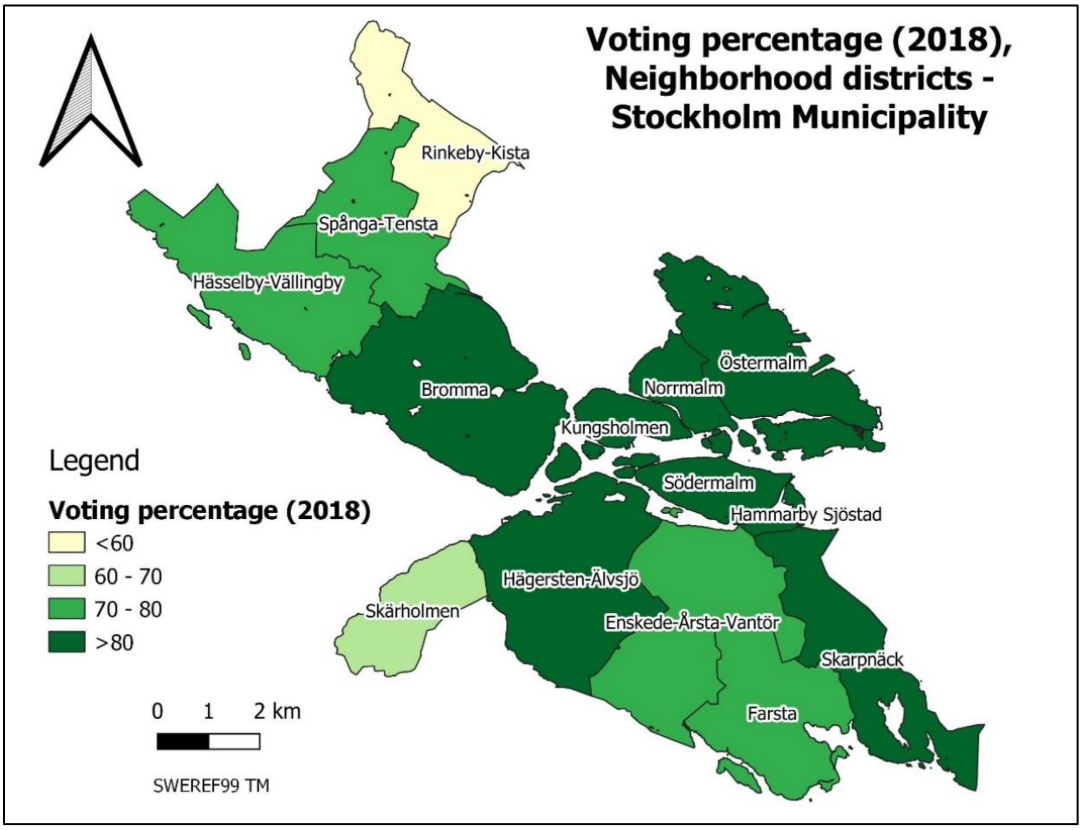

Figure 1. Voting percentage (2018) per Neighborhood district within Stockholm Municipality.

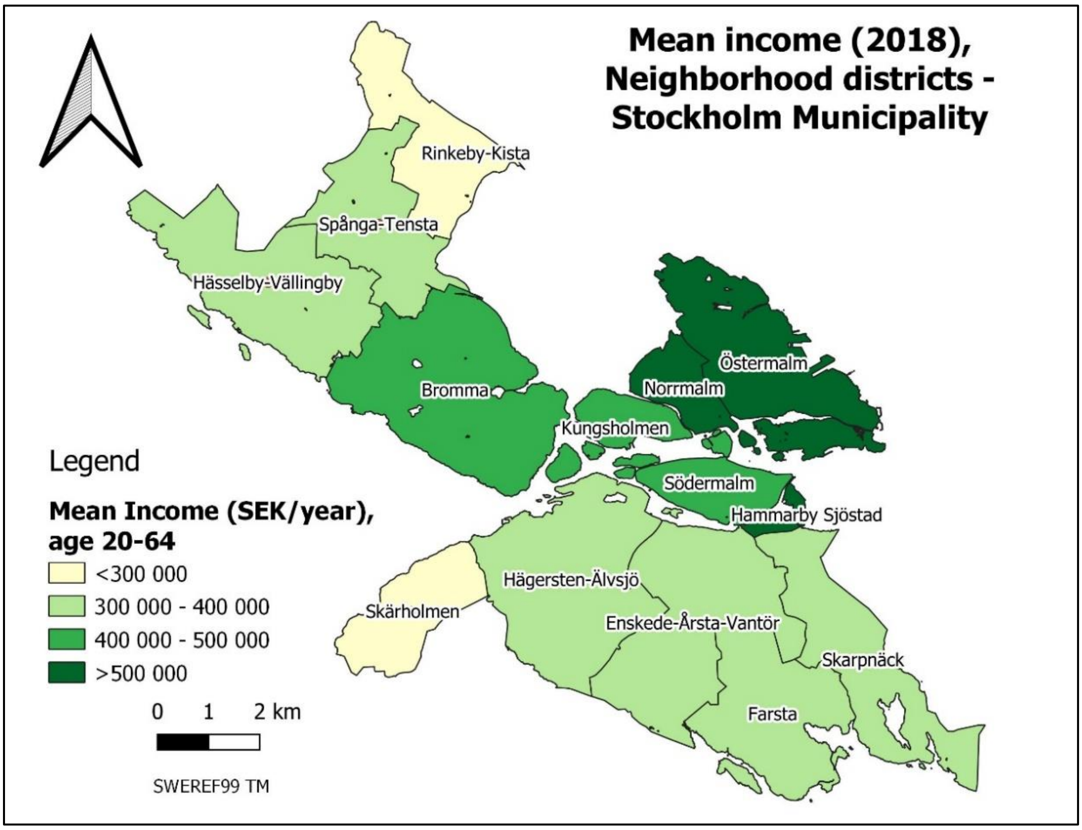

Figure 2. Mean income (SEK/year), age 20-65, as of 2018 for neighborhood districts in Stockholm Municipality.

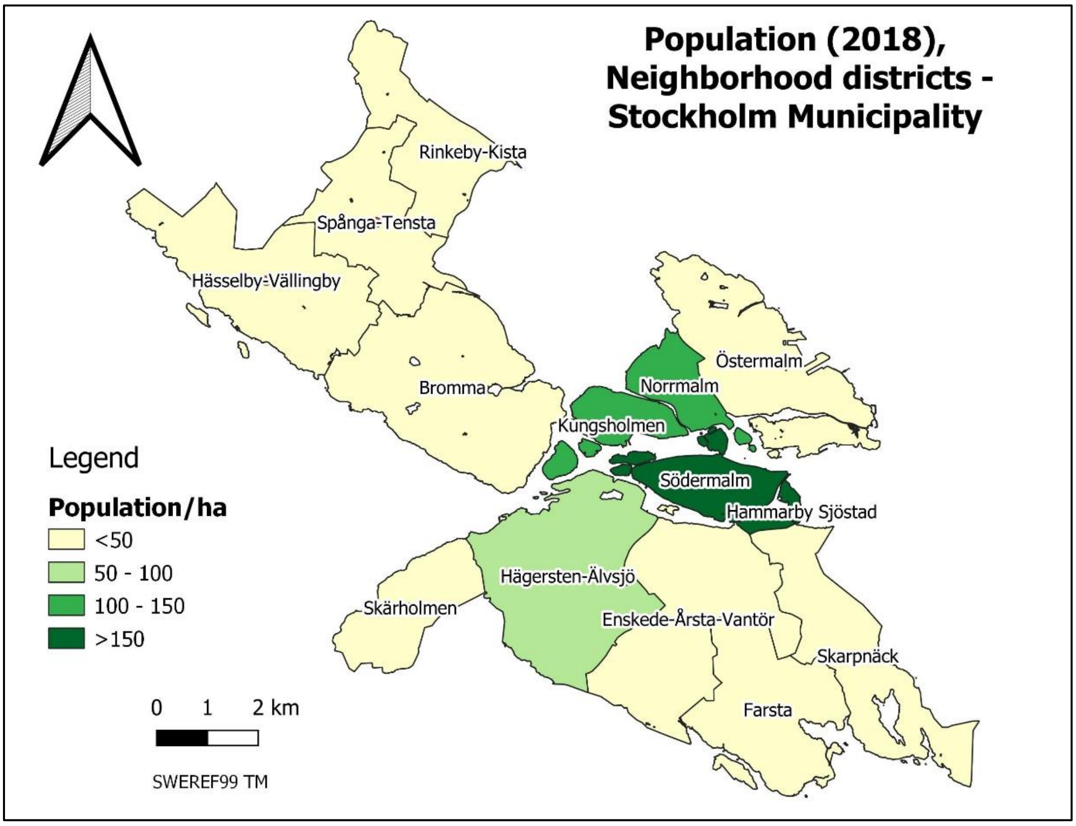

Figure 3. Population per hectare for municipal districts in Stockholm Municipality.

The municipality of Stockholm is divided into several geographically defined administrative entities at different levels. For this study, two geographical administrative divisions are used for aggregating electoral districts to macro-entities. At the coarsest level, the municipality can be divided into three larger areas (*Stadsområden*), namely *'Innerstan'* (Inner-city), *'Västerort'* (western part) and *'Söderort'* (southern part). Nested within these areas, at the local level, are 13 administrative districts (*Stadsdelsområden*) in which the administration of the local welfare is operated (Stockholms Stad, 2021b). Henceforth, the larger areas of Stadsområden are referred to as 'Municipal Districts' and the local Stadsdelsområden as 'Neighborhood districts'. For administrative districts, see Table 1.

In this study, the neighborhood districts were subject to some minor geographical adjustments in order to keep the definition of Innerstan intact with its historical and popular definition in order to be able to incorporate the main islands, and subparts of islands, within the city center. In the southeastern part of the district "Södermalm", the area of "Hammarby-Sjöstad" was separated from its official district to constitute its own. Due to this decision, this study uses 14 neighborhood districts (instead of the 13 official ones) nested within the otherwise intact 3 Municipal Districts. For location of administrative districts, see Figure 4.

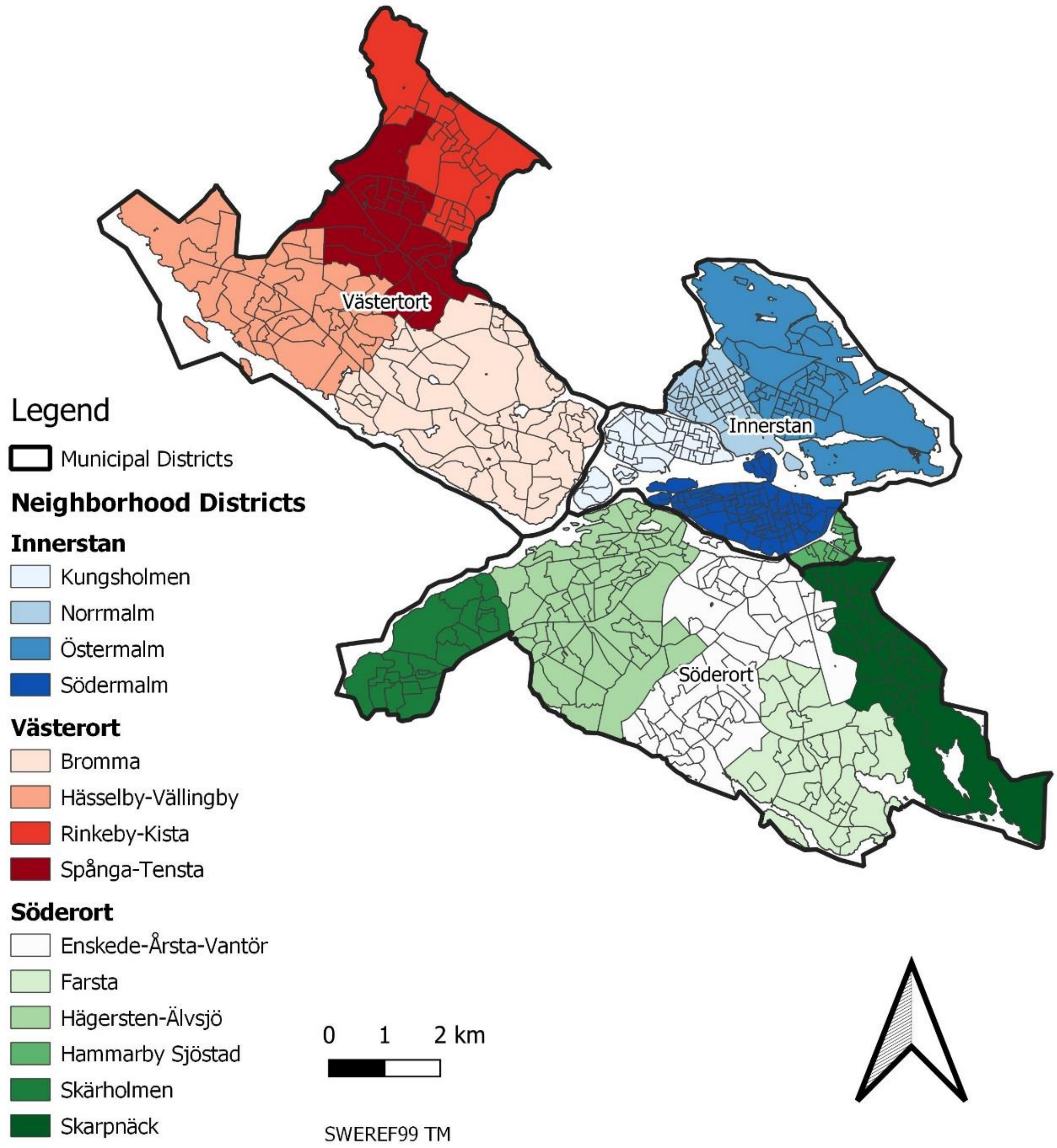

Figure 4. Electoral districts by Neighborhood district within Stockholm Municipality, election year of 2018.

4. Method

The Methodological approach of this thesis is divided into three steps. These can be understood by following the flowchart in Figure 5. The first step consisted of data collection (Box 1). The second step consisted of data preprocessing (Box 2). Importantly, at this stage the electoral districts were attributed election results and subjected to a *retrofitting process* in which historical electoral districts (and results) were harmonized to the electoral districts of 2018. Then two variables based on different political groupings were created. The third step (Box 3) consisted of data analysis of these variables where the first research question (how has the degree of geographic polarization varied for each election?) is addressed by Global Moran's I and the second research question (how has the local degree of geographic polarization varied across the municipality, for each election?) is addressed by Local Moran's I.

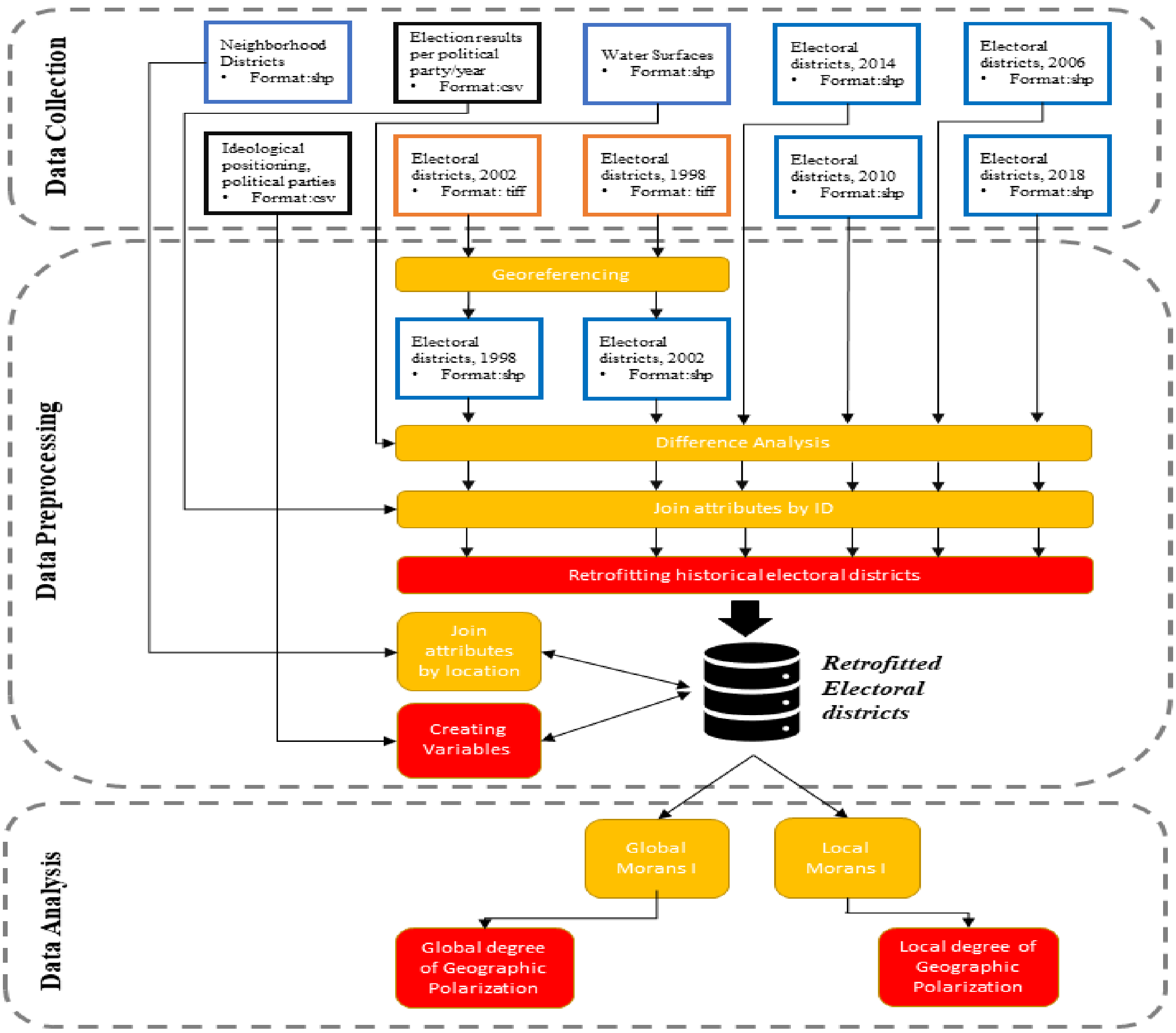

Figure 5. Flowchart describing the process of data collection, data preprocessing and data analysis.

4.1 - Data Collection

Spatial and non-spatial data were gathered from various sources. Geographical information on electoral districts (polygons) were available as shapefiles from the Swedish Election Authority (*Valmyndigheten*) for the election years of 2018, 2014, 2010 and 2006 (Valmyndigheten, 2021b). Geographical information for the elections of 2002 and 1998 do not exist in a digitalized GIS-format and had to be retrieved from the Election committee of Stockholm municipality (*Valnämnd*) as analog maps (Stockholms Valnämnd, 2002; Stockholms Valnämnd, 1998). The analog maps were digitally scanned and stored in tiff-format. For comparison of the electoral districts of 1998 and 2018, see appendix 8.3. Additional GIS-data gathered were Neighborhood Districts of Stockholm Municipality provided by the City Planning office of Stockholm Municipality (Stockholms stad, 2021c) and water surfaces (Ocean and lakes) from the Property Map (*Fastighetskartan*) provided by the Swedish mapping, cadastral and land registration authority (*Lantmäteriet*) (Lantmäteriet, 2021). For a summary of all gathered spatial data, see Table 2.

Table 2. Summary of gathered spatial and non-spatial data.

Type	Data	Format	Source	Scale	Uncertainty
Spatial Data	Electoral districts, 2018	ESRI Shape	Swedish Election Authority	n/a	n/a
	Electoral districts, 2014	ESRI Shape	Swedish Election Authority	n/a	n/a
	Electoral districts, 2010	ESRI Shape	Swedish Election Authority	n/a	n/a
	Electoral districts, 2006	ESRI Shape	Swedish Election Authority	n/a	n/a
	Electoral districts, 2002	Analog Map	Election committee of Stockholm municipality	n/a	n/a
	Electoral districts, 1998	Analog Map	Election committee of Stockholm municipality	n/a	n/a
	Neighborhood districts	ESRI Shape	City planning office, Stockholm municipality	1:4 000 - 1:8 000	10 meter
	Water surfaces	ESRI Shape	Swedish mapping, cadastral and land registration authority	1:5 000 - 1:20 000	10 meter
Non Spatial Data	Election results, 1998- 2018	Csv	Statistics Sweden	n/a	n/a
	Ideological positioning of political parties	Csv	The Swedish National Election Studies	n/a	n/a

Non-spatial data consisted of ideological positioning of political parties and election results from 1998 to 2018 (see Table 2). Ideological positioning of political parties was gathered from reports by the Swedish National Election Studies (*Valforskningsprogrammet*) who have conducted longitudinal surveys on the ideological positions of political parties, according to the Swedish electorate, for every general election since 1979. As of 2018, the survey questionnaire was formulated as:

"In politics, people sometimes talk about left and right. Where would you place the parties on a scale between 0 and 10 where 0 stands for left and 10 stands for right" (Oscarsson & Svensson, 2020 p. 3)

Data from these surveys, for the main political parties (elected to parliament), were gathered from the report by Oscarsson & Svensson (2020). The ideological positioning of *Feministiskt initiativ* (FI), which is not represented in the parliament but has a substantial local following, were gathered from separate reports by Statistics Sweden (SCB; swe: *Statistiska centralbyrån)* (2011), Oscarsson (2016) and Oscarsson (2020). Data on election results per electoral district and political party were gathered from *SCB (2021)*(SCB, 2021).

4.2 – Data Preprocessing

As a first step in the data preprocessing, the tiff-files for election year 2002 and 1998 were georeferenced (see Figure 5). The geoprocessing was facilitated by documents and maps from the Election committee which contained information on new, adjusted, and intact electoral districts, in relation to the previous election. Because of this, geographically intact electoral districts between two elections could be used as safe reference points.

Shapefiles for the electoral districts of 2002 and 1998 were created with the help of the georeferenced tiff-files (see figure 5). This was done by rendering the tiff-file "beneath" the shapefile (of the succeeding election) and manually changing the borders of the shapefile to align with the borders of the tiff-file. The ID of the electoral districts were updated according to the documents from the Election committee. This was done in a stepwise order (the GIS-layer of 2002 was created from a modified version of the GIS-layer of 2006 while 1998 was created from 2002). After this process, six separate GIS-layers with electoral districts for each election year of 2018 (n = 573), 2014 (n = 537), 2010 (n = 503), 2006 (n = 461), 2002 (n = 450) and 1998 (n = 441) were produced.

Areas within electoral districts that overlapped with oceans and lakes were subtracted from the layers using a vector overlay *'Substract* (see Figure 5). This because the areas of the election districts that overlaps with water is arbitrarily drawn for each election. This arbitrary redrawing would therefor affect the accuracy of retrofitting process. Lastly, the electoral districts for each year were attributed data on election results (absolute votes per party) by a common unique ID using *'Join attributes by ID'* (see figure 5).

4.2.1 – Retrofitting historic electoral districts

To harmonize the electoral geography of elections prior to 2018, both the geography and election results were retrofitted to the electoral geography of 2018 (see figure 5). This is the same methodological approach used by Kinsella C. et al. (2015) for harmonizing electoral districts at different elections. Through this method, the 2018 electoral districts were used as a standardized dataset, in which the election result of the previous electoral districts was attributed into depending on the percentage of spatial intersection.

The process of retrofitting a previous election to the 2018 electoral districts consisted of several steps. Firstly, a relationship dataset with a "one-too-many" logic between the 2018 layer and the layer of the previous election was created using *'Join attributes by location'*. Here a duplicate feature of a 2018 electoral district is created for every instance that it intersects with an electoral district of a previous election, inheriting the unique district IDs from both layers in two separate columns. As an example, if one electoral district of 2018 intersects with three districts from a previous election, three features will be created. The column with the ID of 2018 will consist of the same ID while the column with the ID of the previous election consists of the three different IDs.

The percentage intersection between the total area of each 2018 electoral district, to the intersecting ones of the prior election was calculated. This was done by utilizing spatial queries (see appendix 8.1) which stored the percentage overlap (as decimal value) for each feature in the relationship dataset. This decimal value was then multiplied by the total number of votes for each political party for the electoral district prior to 2018. The table is then summed up by the column with the IDs of 2018 and joined to the original GIS-layer with the electoral districts of 2018, ultimately redistributing the values for the prior election result to the geography of 2018. This process was iterated for all historic elections back to 1998. The absolute number of votes per party where then recalculated to the percentage of total votes and stored in a separate column. Lastly, the neighborhood district for each electoral districts was derived by *'Join attributes by location'*(see Figure 5) where they intersected the most.

4.2.2 – Creating variables

Due to Sweden having a multi-party system, the political parties have to be grouped or summed into a single variable before data analysis. Two variables were calculated from the election results of the retrofitted electoral districts (see Table 3). The two variables are: 1) *Percentage left/right margin* and 2) *Ideological voting index.*

The percentage left/right margin variable is calculated as the difference in percentage between the political parties to the left and to the right for each electoral district and year. This creates a theoretical range from +100 (100% margin in votes for left-wing parties) to -100 (100% margin in votes for right-wing parties) at each electoral district. Likewise, if an electoral district has a 50/50 turnout between left- and right-wing parties, the value is 0. As seen in Table 3, for the elections of 1998 to 2018 parties that constitute the left comprise of '*Vänsterpartiet'* (V), '*Feministiskt Initiativ'* (FI), '*Socialdemokraterna'* (S) and *'Miljöpartiet'* (MP). Parties that constitute the right comprise of '*Centerpartiet'* (C), '*Liberalerna'* (L), '*Moderaterna'* (M), '*Kristdemokraterna'* (KD) and '*Sverigedemokraterna'* (SD). Neither parties have ever crossed the "centre-point" of 5 at the ideological dimension, making these party groupings intact for all elections. Percentage left/right margin is formulated as:

$$percentage\ left/right\ margin_{it} = \%(V + FI + S + MP) - \%(C + L + M + KD + SD) \tag{1}$$

Where *it* is electoral district *i* at election year *t*.

Table 3. Ideological positioning of political parties. Values where 0 = Left, 5 = Centre and 10 = Right. The values of SD for year 1998 and 2002 is based on the value of 2006 due to lack of data for these years. Values for FI do not exist for the year of 1998 and 2002 as the party was created in 2005. Data source: SCB (2011), Oscarsson (2016), Oscarsson (2020) and Oscarsson & Svensson (2020).

Year	V	FI	S	MP	C	L	M	KD	SD
1998	1.41	-	3.57	3.75	5.36	6.35	8.85	6.78	7.74*
2002	1.39	-	3.63	3.83	5.71	6.43	8.79	7.08	7.74*
2006	1.34	2.5	3.61	3.55	6.18	6.7	8.4	6.85	7.74
2010	1.25	2.7	3.31	3.86	6.28	6.63	8.31	6.81	7.36
2014	1.4	2.4	3.66	3.87	6.16	6.59	8.22	6.88	7.26
2018	0.83	2.1	3.15	3.02	6	6.5	8.36	7.54	8.29

The Ideological voting index was created by incorporating the ideological position of each party at each specific year (see table 3). This takes into consideration the notion that the partisan vote does not bear the same ideological position at every election as political parties move along the political "left-to-right" dimension (Abrams & Fiorina, 2012). As such, the Ideological voting index sums the ideological position of all votes as by proxy of the party vote of that year. This creates an index ranging from 0 to10 at each election year, for each electoral district. The Ideological voting index was inverted so that high values (close to 10) are considered "left" and low values (close to 0) are considered "right" (i.e. an inversion of Table 3) so that it implies the same logic as percentage left/right margin. The ideological voting index is formulated as:

$$Ideological\,Voting\,Index_{it} = \frac{\sum_p n_{pti} S_{pt}}{\sum_p n_{pti}} * -1 \tag{2}$$

Where *it* is electoral district *i* at election year *t*, *p* is the political party, n_{pti} is the total number of votes (*n*) per *p* at *t* at *i* and S_{pt} is the ideological position (*S*) for *p* at *t*.

4.3 – Data Analysis

To measure the degree of geographical polarization at each election, the dataset was tested for spatial autocorrelation by *Global* and *Local Moran's I*. Global and Local Moran's I are two of the most widely used statistical tools for measuring spatial autocorrelation in areal data (Rogerson, 2001). It has been used to measure geographical polarization by partisan voting on both county (Darmofal & Strickler, 2019) and electoral district-level (Myers, 2013; Kinsella C. et al., ; Kinsella C. et al., 2021). Statistical measurements for both Global and Local Moran's I was calculated in ArcMap 10.5.1.

In the following section, Global Moran's I (Section 4.3.1) corresponds with *research question 1* and Local Moran's I (Section 4.3.2) corresponds to *research question 2.* Lastly, Section 4.3.3 explains the parameters used to conceptualize geographic polarization for both Moran's I computations.

4.3.1 Global degree of Geographic Polarization

To assess the degree of global geographic polarization at an election, Global Moran's I was used. Global Moran's I measures the overall spatial autocorrelation of a variable in a dataset, and to which degree it's spatial structure displays *dispersion*, *randomness* or *clustering* (Rogerson, 2001; ESRI, 2018). For the Global Moran's I computation, see Equation 3.

$$I = \frac{\sum_i^n \sum_j^n w_{ij}(y_i - \bar{y})(y_j - \bar{y})}{(\sum_i^n \sum_j^n w_{ij}) \sum_j^n (y_i - \bar{y})^2} \quad (3)$$

where n is the number of electoral districts, y is the variable of interest and $\bar{y}$ representing it's mean. The values y_i and y_j represents the variable of interest at electoral district i and j with W_{ij} representing the Euclidean distance between electoral district i and j.

The output of global Moran's I is a single value ranging between a theoretical minimum of -1.0 to a theoretical maximum of +1.0. A Moran's *I* value near +1.0 indicate a strong clustered spatial pattern (positive spatial autocorrelation) where high values tend to be located near high values and low values tend to be located near low values. A Moran's *I* value near -1.0 indicates a strong dispersed spatial pattern (negative spatial autocorrelation) where high values tend to be located near low values, and vice versa. Although theoretically possible, a significantly dispersed spatial pattern is very rare and seldom observed. A Moran's *I* near 0 indicates an that there is an absence of spatial pattern, or that the pattern is random. However, the exact value for no spatial autocorrelation is not 0 but an expected value (see Equation 4) that is based upon number of observations (in this case electoral districts).

$$E[I] = \frac{-1}{n - 1} \quad (4)$$

Where E is the expected value of I and n represents the number of electoral districts.

In ArcMap 10.5.1 Global Moran's I computation incorporates a significance test (ESRI, 2018). In this test, the Moran's I is recalculated into a Z-value and compared to p-value in order to examine if the null hypothesis of spatial randomness can be rejected by either a significant dispersion or clustering. In this study, the null hypothesis of spatial randomness is rejected if the confidence level reaches 99% ($p<0.01$).

The Global Moran's I computations were conducted for each election and for both variables. The resulting Moran's I value is interpreted as an indicator of geographic polarization, with its degree depending on its deviation from the expected value. As the computation is done for each election, the degree of geographic polarization can be examined longitudinally for each election between 1998 and 2018.

4.3.2 Local Analysis of Clustering and Outliers

To assess the local degree of geographic polarization for an election, the variables were tested for Local Moran's I. Local Moran's I tests the spatial autocorrelation of a variable and produces a local value for each observation in the dataset (Rogerson, 2001). For the Local Moran's I computation, see Equation 5.

$$I_i = n(y_i - \bar{y}) \sum_{j \neq i} w_{ij}(y_j - \bar{y}) \tag{5}$$

Where *n* is the number of electoral districts, *y* is the variable of interest and $\bar{y}$ representing it's mean. The values y_i and y_j represents the variable of interest at electoral district *i* and *j* with W_{ij} representing the Euclidean distance between electoral district *i* and *j*. I_i is the Morans *I* at location *i*.

The output of Local Moran's I is a decomposed global Moran's I, indicating the local contribution for each observation to the global value (Rogerson, 2001). As global Moran's I indicates the spatial structure at the global level, local Moran's I is essential for examining the heterogeneity and local variations of the dataset. As each observation has its own local statistic, the local Moran's I can be mapped to uncover the location, extent and degree of local clustering hotspots and diverging outliers. As with global Moran's it calculates a value ranging between a theoretical minimum of -1.0 to a theoretical maximum of +1.0 where the absence of spatial pattern is found at its expected value. For the expected value of Local Moran's I, see Equation 6.

$$E[I_i] = \frac{-\sum_{j \neq i} W_{ij}\,(y_j - \bar{y})}{n - 1} \tag{6}$$

Where *E* is the expected value of *Ii* at location *i*, *y* is the variable of interest and $\bar{y}$ representing it's mean. The value *yj* represents the variable of interest at electoral district *j* with *Wij* representing the Euclidean distance between electoral district *i* and *j*.

In ArcMap 10.5.1 Local Moran's I computation incorporates a significance test which is conducted at every observation (ESRI, 2020a). In this test, the local Moran's I is recalculated to a Z-value and compared to p-value to examine to which certainty the null hypothesis of spatial randomness can be rejected. Importantly, the significance test also determines the *spatial association* of each observation i.e. if it is a part of a clustered, dispersed or random pattern. Significantly clustered observations are denoted as either "High-High" (HH) or "Low-Low" (LL), i.e. an observation with a high value amongst other high values, or a low value amongst other low values. Significantly dispersed observations are denoted as either "High-Low" (HL) or "Low-High" (LH) i.e. an observation with a high value amongst low values, or low value amongst high values. Observations with a random spatial association are denoted as "Non-significant" (NS). For each observation by local Moran's I, the null hypothesis of spatial randomness is rejected when the confidence level is above 95% ($p<0.05$). Given the the variables created in section 4.2.2, a *high value* denotes *left-wing voting* and a *low value* correspond with *right wing voting.*

The Local Moran's I computation was conducted on the Percentage left/right margin variable. The local Moran's I Score for each statistically significant electoral district was mapped with the incrementation of +/-0.1 on the Moran's I theoretical scale. The average Moran's I score for statistically significant electoral districts per municipal district and year was calculated. After that, an average Moran's I score for the whole time period was calculated for each municipal district.

4.3.3 – Conceptualizing Geographic Polarization

When testing for spatial autocorrelation by both Global and Local Moran's I, a prerequisite is the conceptualization of spatial relationships for the geographical features and the variable that is tested. A component of Moran's I is it's spatial weight (w_{ij}) where the spatial relationship between observation i and j is conceptualized by a value of spatial proximity (see Equation 3 and Equation 5). An example of a common spatial relationship is the "binary connectivity" in which the value of i is only influenced by the value of j if they are contiguous (Rogerson, 2001). This spatial conceptualization of political polarization has been used for regional studies on county-level in the (Darmofal & Strickler, 2019) and parliament constituencies in UK (Cutts & Webber, 2010) where the distance between the areal center of the observations are large but also relatively varying. However, when analyzing at a fine-scale district-level this is not suitable as districts in the same neighborhood that are not contiguous, but only a few hundred meters apart, would be modeled to have no influence on each other.

The conceptualization of spatial relationships chosen for this study is *Inverse distance* with a *Euclidean distance* method. The Inverse distance concept is defined such as every observation *j*, within a specified threshold distance from *i* is a neighbor of *i*, but nearby observations of *j* have a stronger influence on *i* then far away observations of *j* (ESRI, 2020b). Regarding the analysis on electoral districts, this conceptualization was proposed by Kinsella C. , McTague, Raleigh (2015) with a threshold distance that ensured every electoral district to have at least three neighbors for its Moran's I computation. In this study area, the minimum distance to ensure at least three neighborhoods was 2840.807 meters, hence the chosen threshold distance in this study. Further justifications for this threshold distance were found by an Incremental Spatial Autocorrelation analysis which measures the intensity of spatial autocorrelation of a variable at different Euclidean distances (pro.arcgis.com, 2021). As the peak of Incremental Spatial Autocorrelation suggest the threshold distance where the spatial processes tend to be most clustered, or dispersed, it is often considered an appropriate parameter value as input to the inverse threshold distance. The result from the Incremental spatial Autocorrelation analysis concluded that the spatial autocorrelation by inverse distance was the most pronounced between 2615 to 2972 meters depending on year and variable, hence close to the chosen Euclidean distance of 2840.807 meters in this study.

5. Results and Discussion

In the following section, descriptive results from the retrofitting process on general voting patterns are presented prior to the research questions. Results on the general voting pattern are addressed in section 5.1. Results and discussion regarding the first research question on global degree of polarization is presented in section 5.2. Section 5.3 presents results and discussion on the second research question on local degree of polarization. Lastly, section 5.4 constitute a methodological discussion.

5.1 General voting pattern

Descriptive results from the retrofitting preprocessing show that the voting outcome in Stockholm Municipality is historically right-leaning. Table 4 shows the mean, minimum and maximum values of each variable per year in the dataset comprised of 578 electoral districts. As indicated by the percentage left/right variable, the municipality has voted consistently in favor for right-wing parties, with the only exception being the election year of 2002 where the variable reaches a positive value. The right-wing tendency is also reflected in the ideological voting index as the mean ideological positioning of the vote is slightly below the 'Centre-point' of 5 for each election. As these statistics serve as inputs for the computation of Global and Local Moran's I, the yearly result from both methods is to be understood in relation to these descriptive statistics (e.g. an electoral district which is to the left, or right, is so in relation to the mean of that specific election year).

Table 4. Descriptive statistics the 578 electoral districts used as input for Global and Local Moran's I within Stockholm Municipality.

Variable	Year	Mean	Min	Max
Percentage left/right margin	1998	-1.5	-79.62	75.8
	2002	3.42	-77.19	73.41
	2006	-11.68	-82.46	72.83
	2010	-12.53	-88.37	79.37
	2014	-0.18	-84.57	86.2
	2018	-4.93	-83.51	83.8
Ideological Voting Index	1998	4.48	2.27	6.48
	2002	4.75	2.67	6.39
	2006	4.29	2.47	6.23
	2010	4.35	2.59	6.48
	2014	4.65	2.67	6.35
	2018	4.85	2.53	6.92

5.2 Global degree of Geographic Polarization

The result from Global Moran's I show that the partisan vote is significantly clustered. This is the case for each election and for both examined variables. As table 5 shows, all election years have a p-value lower than 0.01 (1*10E-07) and z-scores higher than 2.58 resulting in less than 1% probability that the pattern could be produced by a random spatial process. At all elections, the Moran's I reaches above the expected Index value of -1.75*10E-3. Due to the similar results for both variables, the shifting of ideological positions by political parties at each election (as highlighted by Abrams & Fiorina (2012)) does not have a substantial impact on the degree of geographic polarization.

Table 5. Global Moran's I for Stockholm Municipality (1998-2018).

Variable	Year	Moran's Index:	Expected Index*10E-3:	z-score:	p-value*10E-07
Percentage left/right margin	1998	0.64	-1.75	78.8	1
	2002	0.61	-1.75	75.2	1
	2006	0.60	-1.75	73.2	1
	2010	0.58	-1.75	71.7	1
	2014	0.63	-1.75	77.5	1
	2018	0.64	-1.75	78.7	1
Ideological Voting Index	1998	0.64	-1.75	78.4	1
	2002	0.62	-1.75	76.2	1
	2006	0.60	-1.75	74.0	1
	2010	0.58	-1.75	71.1	1
	2014	0.63	-1.75	77.7	1
	2018	0.65	-1.75	79.3	1

The degree of clustering varies at each election year. As shown in table 5, the level of Moran's I fluctuates throughout the period showing both an increase and decrease between elections. For both variables this pattern is similar. For percentage left/right margin, the first election of the timeline (1998) has an index-score of 0.64. It then decreases for the subsequent election years of 2002 (i = 0.61), 2006 (i = 0.60) and 2010 (i = 0.58). For the election year of 2014 this pattern is broken, and the Moran's I index score rises to 0.63. For the election year of 2018, the Moran's index-score rose again to 0.64 reaching the same degree of clustering as the peak of 1998. This shows that although the recent election of 2018 did have a relatively high degree of geographic polarization, it is not exceptional from a historic perspective, as it is at a similar degree as at the beginning of the timeline (1998). The result differs from similar local-level analysis in the United States (see e.g., Myers, 2013; Kinsella C. et al., 2015) as it does not indicate a generally increasing polarization process through time, i.e. from relatively *low* to *high* values of Global Moran's index score. To make precise comparisons, in the study by Kinsella C. et al., (2015), Global Moran's index score increased from roughly 0.45 (1976) to a near theoretical maximum of 0.95 (2008). Similarly, Myers (2013) show an almost continuous increase of the Global Moran's I index score, for the change in the Republican vote (compared to the election for 1996) in the state of Texas, rising from 0.30 in 1998 to 0.76 in 2010. The difference in the results between this study and the studies in the United States, may be explained due to differences in urban/rural voting patterns and the spatial extent to which the studies are conducted. It is important to note that the American studies on local-level geographical polarization are all conducted on larger study areas, covering the geographical extent of wider metropolitan areas (Kinsella C. et al., 2015) and entire states (Myers, 2013; Sussell, 2013). Hence these studies comprise of both rural and urban areas, compared to this study, which solely covers the extent of high density urban and sub-urban areas of Stockholm Municipality. As the American party vote (and other social and cultural aspects of life) according to some is increasingly sorted along the urban and the rural (Scala & Johnson, 2017; Johnson & Scala, 2021) a geographic polarization along these lines will show an increase in clustering as shown by Myers, (2013) and Kinsella C. et al., (2015), provided that the study area covers the extent of this spatial process. In this study, with a geographical focus on the urban core rather than a wider metropolitan region, or state, the process of a potential geographic polarization along the urban and rural is not examined. This could perhaps explain the difference in results between this and the American studies, and one can speculate that a study covering the wider metropolitan area of Stockholm would reveal an increasing urban/rural geographic polarization similar to the United States. Obviously, this can only be the case if the suggested urban-rural division of the United States in regard to voting (Scala & Johnson, 2017) is also applicable to Sweden. However, observations on decreasing partisan sorting in relation to the urban and rural divide in Sweden contests this notion (Oscarsson, et al., 2021), as well as the descriptive results from this study that show that the voting outcome in the municipality of Stockholm is fairly even (Although it is historically slightly right-leaning). This is in stark contrasts to the United States where similar sized cities are strongly dominated by the Democratic Party, and the Republican party is relegated to rural areas (Myers, 2013; Kinsella C., et al., 2015; Kinsella C., et al, 2021). Putting the potential sources that may explain the difference in results aside, it is clear that geographic polarization, as a process that is increasing in time, is not as pronounced in Stockholm Municipality as in the Study areas in the United States.

5.3 Local degree of Geographical Polarization

The local degree of clustering varies within the municipality. Figure 6 shows the Local Moran’s I index score between election years of 1998-2018 grouped by spatial association. Most statistically significant clustered electoral districts (HH and LL) show a local Moran’s I score between 0 to +0.1. However, the electoral districts with higher degrees of Moran’s I score are clustered in two areas. For HH-districts it is the neighborhood districts of Spånga-Tensta and Rinkeby-Kista and for LL-districts it is in Norrmalm, Östermalm and Kungsholmen. The spatial pattern of pronounced clustering in these areas is repeated, at various magnitudes, throughout the whole time-period. While no electoral districts within Spånga-Tensta and Rinkeby-Kista reaches an index-score above 0.2, the neighborhood districts of Norrmalm and Östermalm have electoral districts reaching between 0.2-0.3, and for some elections such as 1998, 2002, 2014 and 2018 above >0.3.

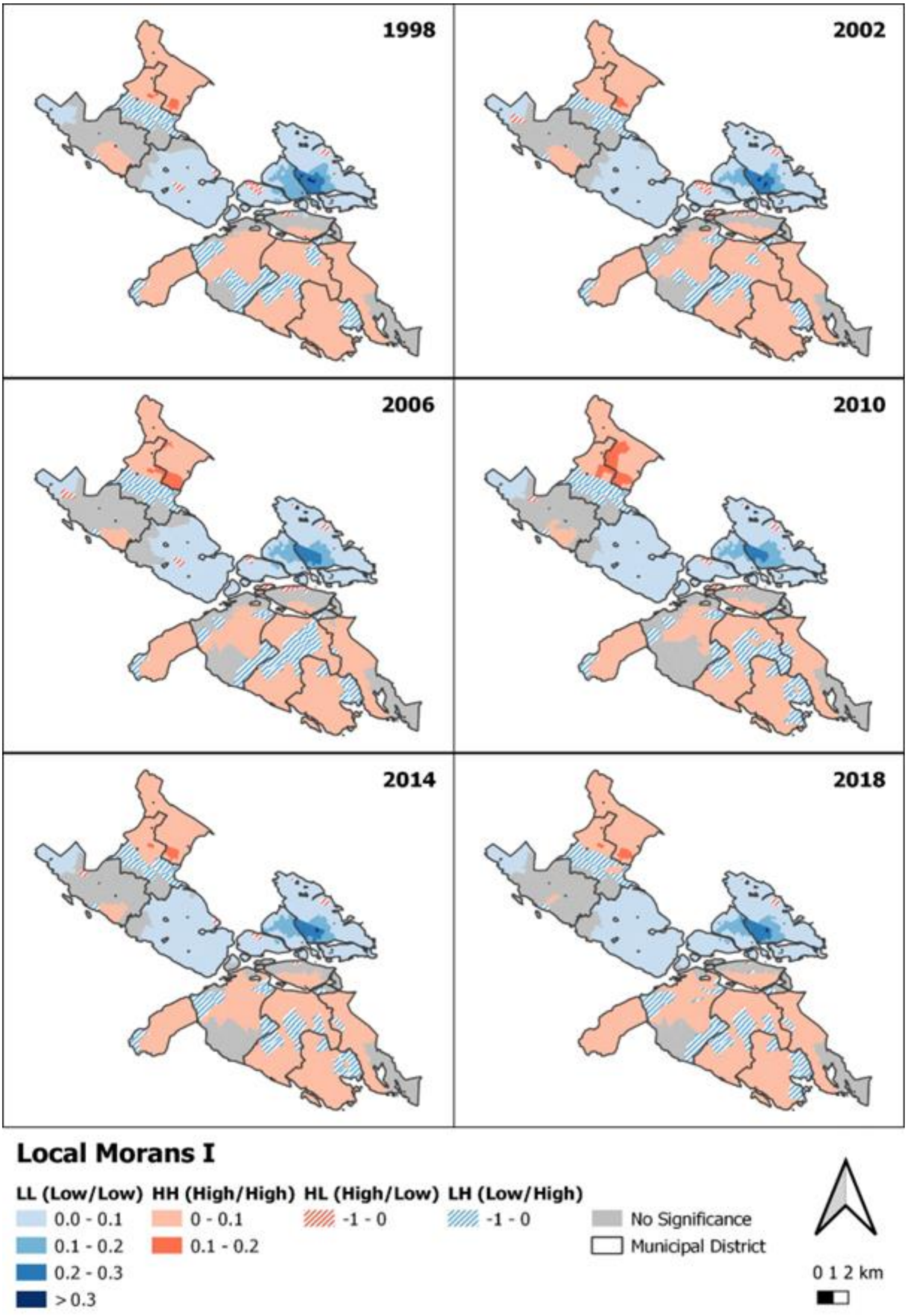

Figure 6. Local Moran's I per electoral district, Stockholm Municipality 1998-2018.

The average degree of clustering varies between the neighborhood districts. Figure 7 show the average Local Moran's I value for statistically significant electoral districts, per year and neighborhood districts, together with an average for the whole time period. The neighborhood districts with the highest degree of clustering is Östermalm with a period average of i = 0.15 followed by Norrmalm with a period average of i = 0.11. After these, in descending order of clustering, is Rinkeby-Kista (period average of i = 0.07), Kungsholmen (period average of i = 0.05), Spånga-Tensta (period average of i = 0.04), Skärholmen (period average of i = 0.03), Skarpnäck (period average of i = 0.02), Bromma (period average of i = 0.02), Enskede-Årsta-Vantör (period average of i = 0.01), Farsta (period average of i = 0.01), Södermalm (period average of i = 0.01) Hägersten Älvsjö (period average of i = 0.01) and Hässelby-Vällingby (period average of i = 0.0). Hammarby-Sjöstad is the only municipal district where the average degree of Local Moran's I, for significant electoral districts, indicate dispersion (period average of i = -0.01).

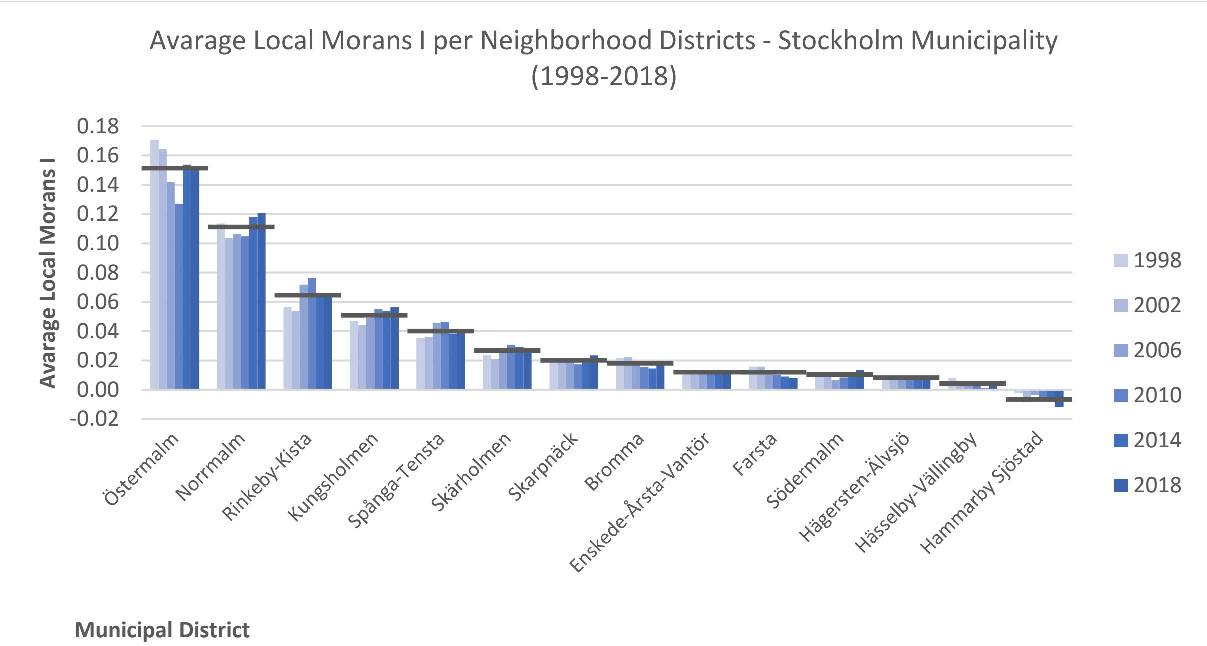

Figure 7. Average Local Moran's I per Neighborhood District and year. The Black bar shows the average Moran's I for 1998-2018.

The right-wing vote is mostly clustered in the central part of the municipality, while the left-wing vote is clustered in the suburbs. This is the case for every election year. As shown in Figure 6, LL-districts dominate the Municipality district of Innerstan with the exception of Södermalm which has a high amount of non-significant and HH-districts. In the municipality districts of Söderort and Västerort, HH-districts is the most frequent except for the neighborhood district of Bromma (For number of electoral districts per Municipal and

Neighborhood District, see Appendix 8.2). This central and peripheral pattern is a similar, but also mirrored, result to studies in the United States. In local-level studies in the United States, the voting pattern is that the Democratic party tends to cluster at densely populated centers while the Republican vote is clustered around it in the periphery of rural or sub-urban areas (Myers, 2013, Kinsella C., et al., 2015,. Johnson & Scala, 2021). In Stockholm municpality this patern is reversed, as it is the right-wing vote that is clustered at the urban core, and the left-wing vote that is clustered in the periphery. However, this notion is only true given the assumption that the Republican party constitute “the right” and the Democrati party constitute “the left”, which may be problematic due to the large local and ideological variation of party representatives, within the two parties (Oscarsson, et al., 2021).

Electoral districts with a dispersed spatial pattern are scattered across the municipality. As Figure 6 shows, a handful of HL-districts are to be found in central part of the municipality (Innerstan) and occasionally to the west (Västerort). A relatively large cluster of HL-districts are located in the northwestern part of Kungsholmen at the election year of 1998 and 2002 which as of the election year 2018 have switched to HH. Compared to HL-districts, the number of LH-districts are larger in number for every election. There are two main areas with LH-districts. To the northwest in Spånga-Tensta, a large uniform cluster of LH-districts is located at each election. The other area is to the south in Söderort where several clusters, or individual electoral districts, are present at each election in various numbers. While these dispersed electoral districts contribute negatively to the Global Moran’s value, making the Global Moran’s I ”less” clustered and geographically polarized, they could still be interpreted to be local examples of geographic polarization. As such, noticeable clusters of dispersed electoral districts such as the one in Spånga-Tensta, should not be interpreted as ”non-polarized” due to being neighbor to the clustered HH-districts of Rinkeby-Kista. Instead, they show polarization towards its own immediate spatial surroundings rather than the global mean as the case for clustered electoral districts.

5.4 Methodological Discussion

5.4.1 MAUP and Retrofitting Electoral Districts.

As with any analysis on aggregate geographical data, the methodological approach in this study is affected by MAUP. With regard to scale, it is best practice to analyze the process being studied at the scale at which it operates (Li, et al., 2018). Theoretically, Bishop (2009) proposed this to be at the local scale of neighborhoods. At the same time, studies show that geographic polarization exists at varying scales, both at micro (e.g. electoral districts) and meso-level (e.g. counties and states). However, the problem surrounding MAUP and scale can be argued as mitigated by analyzing electoral districts compared to e.g. the more aggregated districts such as neighborhood districts. It is clear from the result that despite the fact that some neighborhood districts are homogenous in their voting outcomes (e.g. Norrmalm and Rinkeby-Kista) some areas show variation (e.g. Spånga-Tensta and Enskede-Årsta-Vantör). Hence, aggregate analysis on these neighborhood districts would lead to misleading conclusions, and potential ecological fallacies, as sub-entities within them may deviate radically from the aggregate result.

The impacts of MAUP in regard to zoning are hard to assess. The delineation of geographical data can severely impact the statistics (Wong, 2009) and it cannot be excluded that alternative demarcations of the electoral districts would present different results. The fact that electoral districts change between election years adds further complexity to the zoning-problem. This problem was addressed using the retrofitting-method as previously done by Kinsella C. et al., (2015) which approach was deemed most pragmatic and straight-forward. However, it is built the assumption that different party votes (or groupings of parties) are equally distributed amongst the polygon-features. When half of one electoral district is distributed to another electoral district, half of its votes, regardless of party, gets attributed to that area. Of course, this assumption is false as 1) the voters are not equally distributed amongst the polygon and 2) even the voters where, the specific party vote is most likely not. Even at the local level of electoral districts, spatial variance in regard to voting most likely exists between neighborhood blocks, streets and apartment buildings. Hence, the retrofitting process is akin to the ecological fallacy, as the election result of sub-part of an electoral district is concluded from its aggregate macro-geographical unit.

5.4.2 Moran's I and geographic polarization.

Potential sources of error exist due to the chosen parameters for Moran's I. As geographic polarization of the partisan vote is not a concept of the physical geography (such as trees, rocks etc.) but rather a theoretical concept, to conceptualize it and apply it to the physical world is a challenge. In this study the spatial relationship between electoral districts was conceptualized by Inverse distance with a Euclidean distance method but this can be problematic when the study area is relatively small, such as the case in this study. Due to the chosen threshold distance of 2840.807 meters, the electoral district at the outer fringe has a relatively large portion of their surroundings consisting of “nodata”. The no-data values do not directly affect the Moran’s I computation, but it must be acknowledged that data observations (electoral districts) do exist in these areas but is ignored by the spatial conceptualization, and that their inclusion could have noticeable impact if they would e.g. deviate from its local surroundings.

5.5 Further Research

Studies on geographic polarization of the partisan vote has largely been neglected in Sweden. Hence knowledge of its prevalence and to which degree it manifests at different scales and geographies is unknown. In the United States, a handful of case studies have found evidence of increased geographic polarization at the scale of electoral districts. In this study, no such signs of increased geographic polarization were found. However, compared to the studies in the United States, this study examines the urban-core and suburbs of Stockholm municipality rather than larger metropolitan areas which incorporate both urban and rural areas. Hence, this study does not capture polarization along an urban-rural division as found in the United States. Consequently, the research about geographic polarization within Sweden further studies should emphasize a more regional approach incorporating both urban and rural areas.

Similar research outside Sweden and the United States is emphasized. A limitation of this study is the fact that most similar studies have been conducted in the United States. This is a problem due to the difference in political party system between the countries, making direct result comparisons between them having to be made with caution. Hence, studies on countries with a similar multi-party system to Sweden are very few. An increased number of studies within countries with similar electoral geography and political party system would increase the value of this study as the degree of geographic polarization (which is by some considered a global phenomenon) could be compared across areas, societies and different countries.

The applicability of Moran’s I for measuring geographical polarization have further implications depending on the study area of choice. Intra-municipal analysis, such as this, have challenges related to number of observations (electoral districts) and the problem related to the outer fringe of the study area when using Euclidean distance as a method. Firstly, a general rule for Moran’s I is that the number of observations must exceed 30 to produce any reliable results (ESRI, 2018). This directly limits the applicability to smaller municipalities both within Sweden and abroad as many municipalities have to few electoral districts. Secondly, the usage of Euclidean distance as the spatial conceptualization for measuring polarization inevitably makes data on electoral districts outside the municipality (or other study area of interest) necessary if one wants to retrieve fully reliable results in the outer fringe of the study area. This poses further complications when analyzing historical electoral districts before 2002 as Valmyndigheten do not coordinate electoral districts from municipalities prior to this election. Hence there is a lack of electoral districts prior to 2002 as easily accessible digitized GIS-format. Rather than this, electoral districts before 2002 is provided by the Municipalities themselves in analogue format, with different accessibility and availability depending on municipality. Accessing this historic data that is required to obtain a longitudinal dataset is a time-consuming process. Therefore, national coordination of pre-2002 electoral districts is emphasized as it would facilitate longitudinal time series between historical and future elections.

There is room for methodological improvement in regard to measuring the degree of polarization longitudinally. A key topic and methodological problem is the frequent redrawing of electoral districts at each election. A different methodological approach than the one applied in this study would be to use a high-resolution grid, that is intact for each election, and attribute the absolute number of votes to them from spatially overlapping electoral districts. This would create a spatial dataset, longitudinally intact at each election, but with the absolute number of votes per party inherited from the electoral districts. This could perhaps be a better spatial representation of the vote than using the latest election (in this case the election of 2018).

The methodology of this study also has applicability in research outside the topic of geographic and political polarization. As an example, another political and social problem is the absence of voting and it is clear that low-income neighborhoods also have low voter-turnout (see, table 1). Consequently, this methodology can be further used as an identification tool for geographically clustered societal problems, not only by examining the geographic polarization of the vote in an area, but also high degrees of non-voting. Once areas are identified, further analysis involving additional socio-demographic variables can be conducted, yielding insightful situational awareness for Municipalities in regard to societal issues such as segregation, inequality and marginalization. This may be further used in strategical planning for municipalities to proactively prevent these issues from escalating, hence this methodology can function as an important tool in the work increasing the general welfare of society.

6. Conclusion

Between the election years of 1998 to 2018, Stockholm municipality has had a persistent degree of geographic polarization, with small variations between elections. For all election years the tendency for the left- or rightwing vote to cluster amongst electoral districts is evident. But the degree in which this spatial pattern manifests itself show no unambiguous increase or decrease through time. The degree of geographic polarization was at its lowest at the election year of 2010 and at its highest in 1998 and 2018. This contrast both views within the political debate on increased polarization as well as empirical evidence from the United States that supports it. Hence, the debate surrounding the "Big Sort Hypothesis" and claims of the recent decades elections as increasingly polarized are not strongly manifest within Stockholm Municipality.

Regarding the local degree of polarization across the municipality, the tendency for the right- or leftwing vote to cluster varies. Geographically, the strongest clustering of left-wing votes is located in the suburbs of Spånga-Tensta and Rinkeby-Kista while the strongest clustering of right-wing vote (which is also at a stronger degree) is located in the inner-city of Norrmalm, Östermalm and Kungsholmen. It is clear that these areas constitute the main "poles" in the geographically polarized municipality, and from a temporal perspective this patterns has repeated itself for all elections since 1998. Outlier electoral districts with a dispersed pattern have been identified. Right-wing electoral districts, amongst otherwise left-wing electoral districts, are located in Spånga-Tensta and scattered around Söderort. Historically, the northwestern part of Kungsholmen had several left-wing electoral districts, amongst otherwise ring-wing electoral districts, but as of 2018 these have disappeared.

Evidence of increased geographic polarization was not found at the scale of electoral districts within this study area. The notion that the municipality is more geographically polarized today than in previous elections cannot be supported. However, due to the importance that scale and spatial extent plays in studies on geographic polarization, justification for further studies do exist both in the case of Stockholm and nationwide. In Stockholm, a similar local-level analysis but with a wider regional emphasis (e.g. greater Stockholm metropolitan area) to encompass potential geographical polarization along the urban and rural is emphasized. Nationwide, knowledge to which degree geographic polarization manifests at different scales (e.g. regional, municipal and at electoral district) is unknown. Hence a nationwide examination covering multiple scales (e.g. by multi-level-modeling) would give insightful knowledge on to which degree geographic polarization manifests itself at different scales in Sweden as a whole. Also, it can be concluded that the methodological approach of this study can be used as an identification tool for municipalities when localizing areas that show a high degree of geographic polarization. This in turn, might give insightful knowledge on potential segregation within the municipality. However, the method is not solely limited to localizing geographic polarization of the vote but may also have other fruitful applications, suggestively the localization of areas with a high degree of non-voting.

7 References

Abrams, S. J., & Fiorina, M. P. (2012). "The Big Sort" That Wasn't: A Skeptical Reexamination. *PS: Political Science and Politics , April 2012, Vol. 45, No. 2*, 203-210.

Bishop, B. (2009). *The Big Sort: Why the clustering of likeminded likeminded America is tearing us apart.* Boston: First Mariner Books.

Böttcher, L., & Gersbach, H. (2020). *The great divide: drivers of polarization in the US public.* EPJ Data Sci. 9, 32.

Carothers, T., & O'Donohue, A. (2019). *Democracies Divided: The Global Challenge of Political Polarization.* Brookings Institution Press.

Cutts, D., & Webber, D. J. (2010). Voting patterns, party spending and space in England and Wales. *Regional Studies, Vol. 44*, 735-760.

Darmofal, D., & Strickler, R. (2019). *Demography, Politics, and Partisan Polarization in the United States, 1828–2016.* Springer Nature Switzerland.

DiMaggio, P., Evans, J., & Bryson, B. (1998). Have Americans Social attitudes Become More Polarized. *Princeton University* .

ESRI. (2018). *How Spatial Autocorrelation (Global Moran's I) works*. Retrieved from https://desktop.arcgis.com/en/arcmap/10.3/tools/spatial-statistics-toolbox/h-how-spatial-autocorrelation-moran-s-i-spatial-st.htm

ESRI. (2020a). *Cluster and Outlier Analysis (Anselin Local Moran's I) (Spatial Statistics)*. Retrieved from https://pro.arcgis.com/en/pro-app/2.8/tool-reference/spatial-statistics/cluster-and-outlier-analysis-anselin-local-moran-s.htm

ESRI. (2020b). *Modeling spatial relationships*. Retrieved from https://pro.arcgis.com/en/pro-app/latest/tool-reference/spatial-statistics/modeling-spatial-relationships.htm

ESRI. (2021). *Incremental Spatial Autocorrelation (Spatial Statistics)*. Retrieved from https://pro.arcgis.com/en/pro-app/latest/tool-reference/spatial-statistics/incremental-spatial-autocorrelation.htm

Fiorina, M. P., & Abrams, S. J. (2008). Political Polarization in the American Public. *Annual Review of Political Science*, 563–588.

Forest, B. (2017). Electoral geography: From mapping votes to representing power. *Geography Compass 12*, 1-17.

Johnson, K. M., & Scala, J. D. (2021). *The Rural-Urban Continuum of Polarization: Understanding the Geography of the 2018 Midterms.* The Forum 2021; 18(4): 607–626.

Johnston, R., Jones, K., & Manley, D. (2016). The Growing Spatial Polarization of Presidential Voting in the United States, 1992-2012: Myth or Reality? *Political Science & Politics, 49(4)*, 755-770.

Johnston, R., Jones, K., Propper, C., Burgess, S., & Bolster , A. (2004). Party support and the neighbourhood effect: Spatial polarisation of the British electorate, 1991–2001. *Political Geography* , 367–402.

Johnston, R., Manley, D., Jones, K., & Rohla, R. (2020). The geographical polarization of the American electorate: a country of increasing electoral landslides? *GeoJournal*, 187–204.

Kinsella, C., McTague, C., Raleig, K., & b. (2021). Closely and deeply divided: Purple counties in the 2016 presidential election. *Applied Geography 127*.

Kinsella, C., McTague, C., Raleigh, K. N., & a. (2015). Unmasking geographic polarization and clustering: A micro-scalar analysis of partisan voting behavior. *Applied Geography 62*, 404-419.

Knutson, M. (2019, December 17). *Analys: "Ökad polarisering kan underminera tilltron till demokratin"*. Retrieved from SVT Nyheter: https://www.svt.se/nyheter/inrikes/analys-okad-polarisering-kan-underminera-tilltron-till-demokratin

Lang, C., & Pearson-Merkowitz, S. (2015). Partisan sorting in the United States, 1972e2012: New evidence from a dynamic analysis. *Political Geography 48*, 119-129.

Lantmäteriet. (2021). *Fastighetsindelning Nedladdning, vektor*. Retrieved from https://www.lantmateriet.se/sv/geodata/vara-produkter/produktlista/fastighetsindelning-nedladdning-vektor/

Levendusky, M. (2009). *How Liberals Became Democrats and Conservatives Became Republicans.* Chicago Studies in American Politics.

Li, L., Ban, H., Wechsler, S. P., & Xu, B. (2018). Spatial Data Uncertainty. In *Comprehensive Geographic Information Systems* (pp. 313-340). Elsevier Reference Collection.

Mason, L. (2015). "I Disrespectfully Agree": The Differential Effects of Partisan Sorting on Social and Issue Polarization. *American Journal of Political Science 59(1):*, 128-145.

McKee, S. C., & Teigen, J. M. (2009). Probing the reds and blues: Sectionalism and voter location in the 2000 and 2004 U. S. presidential elections. *Political Geography*, 484–495.

Michaud, J., Mäkinen, I. H., Szilva, A., & Frisk, E. (2021). A spatial analysis of parliamentary elections in Sweden 1985–2018. *Applied Network Science*.

Morrill, R. L., & Webster, G. R. (2015). Spatial and political realignment of the U.S. electorate, 1988e2012. *Political Geography 48*, 93-107.

Morrill, R., Knopp, L., & Brown, M. (2011). Anomalies in Red and Blue II: Towards an understanding of the roles of setting, values, and demography in the 2004 and 2008 U.S. presidential elections. *Political Geography 30*, 153-168.

Myers, A. S. (2013). Unmasking geographic polarization and clustering: A micro-scalar analysis of partisan voting behavior. *Electoral Studies 32*, 48–62.

O'Loughlin, J., Vladimir, K., & Olga, V. (1997). The Electoral Geographies of a Polarizing City: Moscow, 1993-1996. *Post-Soviet Geography and Economics, 38:10*, 567-600.

Oscarsson, H. (2016). Flytande väljare, Statistics Sweden, Democracy Statistics Report no 21.

Oscarsson, H. (2020). Flytande väljare 2018. *Valforskningsprogrammet*.

Oscarsson, H., & Svensson, R. (2020). *Partiernas vänster-högerpositioner 1968-2019. Valforskningsprogrammets rapportserie 2020:2.* Göteborgs universitet: Statsvetenskapliga institutionen.

Oscarsson, H., Bergman, T., Bergström, A., & Hellström, J. (2021). *Demokratirådets rapport 2021: Polarisering i Sverige.* Demokratirådets rapport 2021: Polarisering i Sverige.

Pattie, C., & Johnston, R. (2009). Electoral Geography. *International Encyclopedia of Human Geography*.

Rogerson, P. A. (2001). *Statistical Methods for Geography.* Sage Publications.

Ryne Rohlaa, R., Johnston, R., Jones, K., & Manley, D. (2018). Spatial scale and the geographical polarization of the American electorate. *Political Geography 65*, 117–122.

Scala, D. J., & Johnson, K. M. (2017). Political Polarization along the Rural-Urban Continum. *The Annals of the American Academy of Political and Social Science*, 162-184.

SCB. (2011). *The Eight Parties Election 2010.* Åttapartivalet 2010. Allmänna valen, Valundersökningen.

SCB. (2021). *Allmänna val, valresultat*. Retrieved from https://www.scb.se/hitta-statistik/statistik-efter-amne/demokrati/allmanna-val/allmanna-val-valresultat/

SFS (2005:837). *Vallag [SFS The Elections Act]*. Retrieved from https://www.riksdagen.se/sv/dokument-lagar/dokument/svensk-forfattningssamling/vallag-2005837_sfs-2005-837

Shanto, I., Lelkes, Y., Levundsky, M., Malhotra, N., & Westwood, S. (2019). The Origins and Consequences of Affective Polarization in the United States. *Annual Review of Political Science 22:*, 129–146.

Stockholms Stad. (2019). *Områdesfakta Södra Hammarbyhamnen.* Stockholms Stad.

Stockholms Stad. (2020). *Statistical Year-book of Stockholm 2020.* Stockholms Stad.

Stockholms Stad. (2021a). *Statistical Year-book of Stockholm 2021.* Stockholms Stad.

Stockholms Stad. (2021b). *Stadsdelsförvaltningar*. Retrieved from https://start.stockholm/om-stockholms-stad/organisation/stadsdelsforvaltningar/

Stockholms stad. (2021c). *Öppna data - Dataportalen*. Retrieved from https://dataportalen.stockholm.se/dataportalen/

Stockholms Valnämnd. (1998). Valdistrikt och Vallokaler vid valen 1998. Stockholms stad.

Stockholms Valnämnd. (2002). Valdistrikt och Vallokaler vid valen 2002. Stockholms stad.

Storey, D. (2009). *Political Geography.* University of Worcester, Worcester, UK: Elsevier.

Sussell, J. (2013). New Support for the Big Sort Hypothesis: An Assessment of Partisan Geographic Sorting in California, 1992-2010. *PS: Political Science and Politics*, 768-773. Retrieved from New Support for the Big Sort Hypothesis: An Assessment of Partisan Geographic

Valmyndigheten. (2021a). *The fundamentals of the electoral system*. Retrieved from https://www.val.se/servicelankar/servicelankar/otherlanguages/englishengelska/electoralsystem/generalelections.4.1dac782216e1e29d7891861.html

Valmyndigheten. (2021b). *Valresultat*. Retrieved from https://www.val.se/valresultat.html

Von Arnold, C. (2021, February 01). *Ökad politisk polarisering inte nödvändigtvis av ondo*. Retrieved from Lunds Universitet: https://www.lu.se/artikel/okad-politisk-polarisering-inte-nodvandigtvis-av-ondo

Walks, A. (2005). City-Suburban Electoral Polarization in Great Britain, 1950-2001. *Transactions of the Institute of British Geographers*, 500-517.

Wong, D. (2009). Modifiable Areal Unit Problem.

8. Appendix

8.1 Queries

```
round(area(intersection($geometry, geometry(get_feature('stockholm_2018', '2018_district_id',
"2018_district_id"))))/ area($geometry),2)
```

8.2 Tables

	Bromma					Enskede-Årsta-Vantör					Farsta				
	HH	**LL**	**HL**	**LH**	**NS**	**HH**	**LL**	**HL**	**LH**	**NS**	**HH**	**LL**	**HL**	**LH**	**NS**
1998	0	35	2	0	14	50	0	0	9	0	31	0	0	4	0
2002	0	37	1	0	13	51	0	0	8	0	32	0	0	3	0
2006	0	38	1	0	12	46	0	0	13	0	30	0	0	5	0
2010	0	43	0	0	8	48	0	0	11	0	28	0	0	7	0
2014	0	41	1	0	9	51	0	0	8	0	30	0	0	5	0
2018	0	43	0	0	8	51	0	0	8	0	29	0	0	6	0
	Hägersten-Älvsjö					**Hammarby-Sjöstad**					**Hässelby-Vällingby**				
	HH	**LL**	**HL**	**LH**	**NS**	**HH**	**LL**	**HL**	**LH**	**NS**	**HH**	**LL**	**HL**	**LH**	**NS**
1998	45	0	0	11	14	0	0	0	2	9	7	2	0	1	33
2002	37	0	0	12	21	0	0	0	2	9	5	2	1	1	34
2006	34	0	0	8	28	0	0	0	1	10	2	2	1	1	37
2010	27	0	0	8	35	0	0	0	1	10	3	3	1	1	35
2014	37	0	0	12	21	0	0	0	2	9	1	3	1	1	37
2018	41	0	0	12	17	0	0	0	2	9	2	3	0	1	37
	Kungsholmen					**Norrmalm**					**Östermalm**				
	HH	**LL**	**HL**	**LH**	**NS**	**HH**	**LL**	**HL**	**LH**	**NS**	**HH**	**LL**	**HL**	**LH**	**NS**
1998	0	40	5	0	0	0	44	0	0	0	0	46	1	0	0
2002	0	40	5	0	0	0	44	0	0	0	0	45	2	0	0
2006	0	42	3	0	0	0	44	0	0	0	0	45	2	0	0
2010	0	44	1	0	0	0	44	0	0	0	0	45	2	0	0
2014	0	42	1	0	2	0	44	0	0	0	0	45	2	0	0
2018	0	44	0	0	1	0	44	0	0	0	0	45	2	0	0
	Rinkeby-Kista					**Skärholmen**					**Skarpnäck**				
	HH	**LL**	**HL**	**LH**	**NS**	**HH**	**LL**	**HL**	**LH**	**NS**	**HH**	**LL**	**HL**	**LH**	**NS**
1998	27	0	0	0	0	21	0	0	1	0	26	0	0	0	1
2002	27	0	0	0	0	21	0	0	1	0	26	0	0	0	1
2006	27	0	0	0	0	21	0	0	1	0	24	0	0	1	2
2010	27	0	0	0	0	21	0	0	1	0	24	0	0	2	1
2014	27	0	0	0	0	21	0	0	1	0	25	0	0	1	1
2018	27	0	0	0	0	22	0	0	0	0	25	0	0	1	1
	Södermalm					**Spånga-Tensta**					**Stockholm Municipality**				
	HH	**LL**	**HL**	**LH**	**NS**	**HH**	**LL**	**HL**	**LH**	**NS**	**HH**	**LL**	**HL**	**LH**	**NS**
1998	13	6	2	0	50	10	0	0	8	3	230	173	10	36	124
2002	22	2	5	0	42	10	0	0	7	4	231	170	14	34	124
2006	10	2	6	0	53	10	0	0	8	3	204	173	13	38	145
2010	16	3	4	0	48	10	0	0	8	3	204	182	8	39	140
2014	27	2	2	0	40	11	0	0	7	3	230	177	7	37	122
2018	30	2	1	1	37	12	0	0	6	3	239	181	3	37	113
	Innerstan					**Västerort**					**Söderort**				
	HH	**LL**	**HL**	**LH**	**NS**	**HH**	**LL**	**HL**	**LH**	**NS**	**HH**	**LL**	**HL**	**LH**	**NS**
1998	13	136	8	0	50	44	37	2	9	50	173	0	0	27	24
2002	22	131	12	0	42	42	39	2	8	51	167	0	0	26	31
2006	10	133	11	0	53	39	40	2	9	52	155	0	0	29	40
2010	16	136	7	0	48	40	46	1	9	46	148	0	0	30	46
2014	27	133	5	0	42	39	44	2	8	49	164	0	0	29	31
2018	30	135	3	1	38	41	46	0	7	48	168	0	0	29	27

8.3 Figures

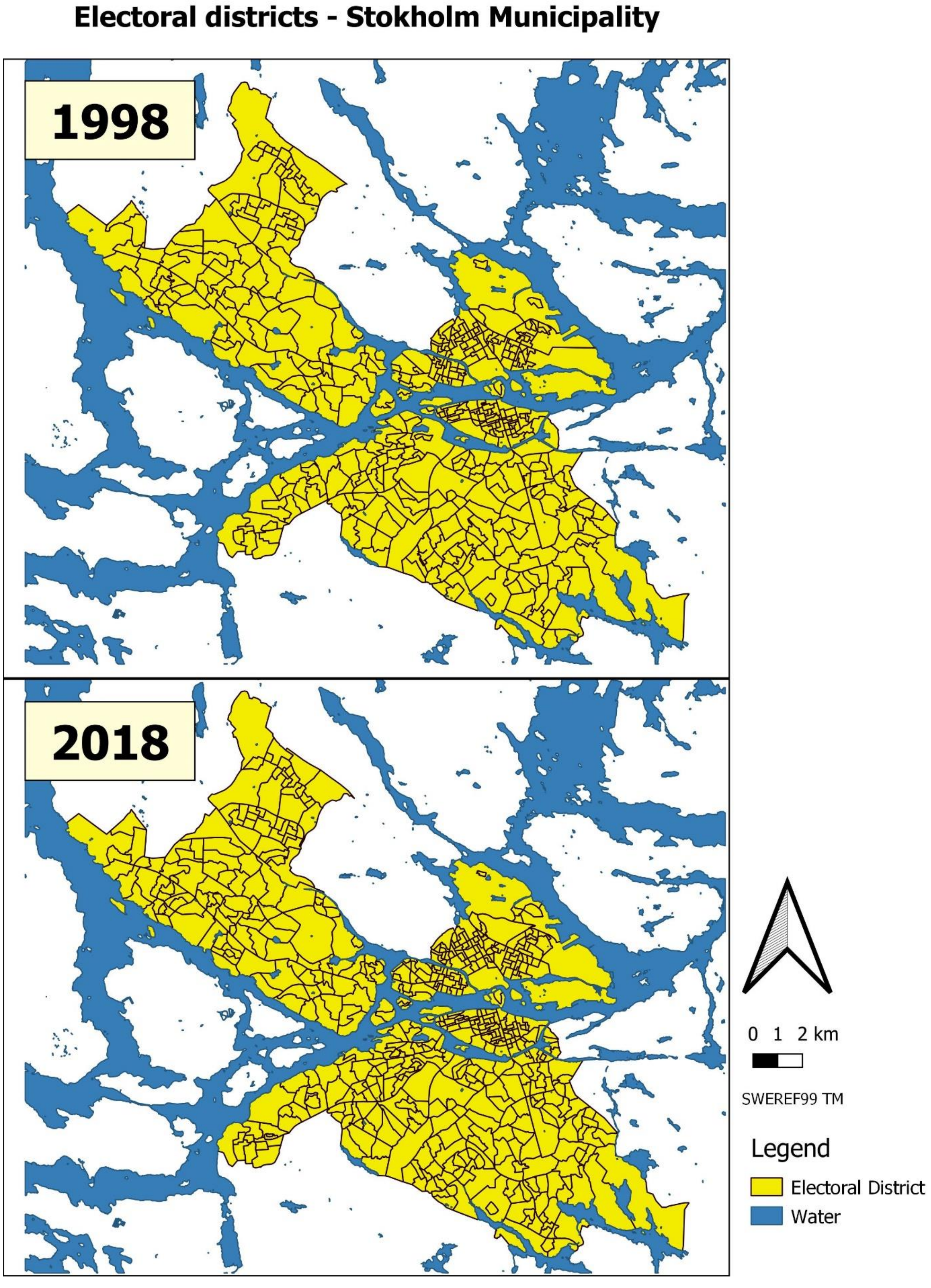

Electoral districts - Stokholm Municipality
1998
2018
0 1 2 km
SWEREF99 TM
Legend
Electoral District
Water

Series from Lund University

Department of Physical Geography and Ecosystem Science

Master Thesis in Geographical Information Science

1. *Anthony Lawther:* The application of GIS-based binary logistic regression for slope failure susceptibility mapping in the Western Grampian Mountains, Scotland (2008).
2. *Rickard Hansen:* Daily mobility in Grenoble Metropolitan Region, France. Applied GIS methods in time geographical research (2008).
3. *Emil Bayramov:* Environmental monitoring of bio-restoration activities using GIS and Remote Sensing (2009).
4. *Rafael Villarreal Pacheco:* Applications of Geographic Information Systems as an analytical and visualization tool for mass real estate valuation: a case study of Fontibon District, Bogota, Columbia (2009).
5. *Siri Oestreich Waage:* a case study of route solving for oversized transport: The use of GIS functionalities in transport of transformers, as part of maintaining a reliable power infrastructure (2010).
6. *Edgar Pimiento:* Shallow landslide susceptibility – Modelling and validation (2010).
7. *Martina Schäfer:* Near real-time mapping of floodwater mosquito breeding sites using aerial photographs (2010).
8. *August Pieter van Waarden-Nagel:* Land use evaluation to assess the outcome of the programme of rehabilitation measures for the river Rhine in the Netherlands (2010).
9. *Samira Muhammad:* Development and implementation of air quality data mart for Ontario, Canada: A case study of air quality in Ontario using OLAP tool. (2010).
10. *Fredros Oketch Okumu*: Using remotely sensed data to explore spatial and temporal relationships between photosynthetic productivity of vegetation and malaria transmission intensities in selected parts of Africa (2011).
11. *Svajunas Plunge:* Advanced decision support methods for solving diffuse water pollution problems (2011).
12. *Jonathan Higgins:* Monitoring urban growth in greater Lagos: A case study using GIS to monitor the urban growth of Lagos 1990 - 2008 and produce future growth prospects for the city (2011).
13. *Mårten Karlberg:* Mobile Map Client API: Design and Implementation for Android (2011).
14. *Jeanette McBride:* Mapping Chicago area urban tree canopy using color infrared imagery (2011).
15. *Andrew Farina:* Exploring the relationship between land surface temperature and vegetation abundance for urban heat island mitigation in Seville, Spain (2011).

16. *David Kanyari*: Nairobi City Journey Planner: An online and a Mobile Application (2011).

17. *Laura V. Drews:* Multi-criteria GIS analysis for siting of small wind power plants - A case study from Berlin (2012).

18. *Qaisar Nadeem:* Best living neighborhood in the city - A GIS based multi criteria evaluation of ArRiyadh City (2012).

19. *Ahmed Mohamed El Saeid Mustafa:* Development of a photo voltaic building rooftop integration analysis tool for GIS for Dokki District, Cairo, Egypt (2012).

20. *Daniel Patrick Taylor*: Eastern Oyster Aquaculture: Estuarine Remediation via Site Suitability and Spatially Explicit Carrying Capacity Modeling in Virginia's Chesapeake Bay (2013).

21. *Angeleta Oveta Wilson:* A Participatory GIS approach to *unearthing* Manchester's Cultural Heritage '*gold mine'* (2013).

22. *Ola Svensson:* Visibility and Tholos Tombs in the Messenian Landscape: A Comparative Case Study of the Pylian Hinterlands and the Soulima Valley (2013).

23. *Monika Ogden:* Land use impact on water quality in two river systems in South Africa (2013).

24. *Stefan Rova:* A GIS based approach assessing phosphorus load impact on Lake Flaten in Salem, Sweden (2013).

25. *Yann Buhot:* Analysis of the history of landscape changes over a period of 200 years. How can we predict past landscape pattern scenario and the impact on habitat diversity? (2013).

26. *Christina Fotiou:* Evaluating habitat suitability and spectral heterogeneity models to predict weed species presence (2014).

27. *Inese Linuza:* Accuracy Assessment in Glacier Change Analysis (2014).

28. *Agnieszka Griffin:* Domestic energy consumption and social living standards: a GIS analysis within the Greater London Authority area (2014).

29. *Brynja Guðmundsdóttir:* Detection of potential arable land with remote sensing and GIS - A Case Study for Kjósarhreppur (2014).

30. *Oleksandr Nekrasov:* Processing of MODIS Vegetation Indices for analysis of agricultural droughts in the southern Ukraine between the years 2000-2012 (2014).

31. *Sarah Tressel:* Recommendations for a polar Earth science portal in the context of Arctic Spatial Data Infrastructure (2014).

32. *Caroline Gevaert:* Combining Hyperspectral UAV and Multispectral Formosat-2 Imagery for Precision Agriculture Applications (2014).

33. *Salem Jamal-Uddeen:* Using GeoTools to implement the multi-criteria evaluation analysis - weighted linear combination model (2014).

34. *Samanah Seyedi-Shandiz:* Schematic representation of geographical railway network at the Swedish Transport Administration (2014).

35. *Kazi Masel Ullah:* Urban Land-use planning using Geographical Information System and analytical hierarchy process: case study Dhaka City (2014).

36. *Alexia Chang-Wailing Spitteler:* Development of a web application based on MCDA and GIS for the decision support of river and floodplain rehabilitation projects (2014).

37. *Alessandro De Martino:* Geographic accessibility analysis and evaluation of potential changes to the public transportation system in the City of Milan (2014).

38. *Alireza Mollasalehi:* GIS Based Modelling for Fuel Reduction Using Controlled Burn in Australia. Case Study: Logan City, QLD (2015).

39. *Negin A. Sanati:* Chronic Kidney Disease Mortality in Costa Rica; Geographical Distribution, Spatial Analysis and Non-traditional Risk Factors (2015).

40. *Karen McIntyre:* Benthic mapping of the Bluefields Bay fish sanctuary, Jamaica (2015).

41. *Kees van Duijvendijk:* Feasibility of a low-cost weather sensor network for agricultural purposes: A preliminary assessment (2015).

42. *Sebastian Andersson Hylander:* Evaluation of cultural ecosystem services using GIS (2015).

43. *Deborah Bowyer:* Measuring Urban Growth, Urban Form and Accessibility as Indicators of Urban Sprawl in Hamilton, New Zealand (2015).

44. *Stefan Arvidsson:* Relationship between tree species composition and phenology extracted from satellite data in Swedish forests (2015).

45. *Damián Giménez Cruz*: GIS-based optimal localisation of beekeeping in rural Kenya (2016).

46. *Alejandra Narváez Vallejo:* Can the introduction of the topographic indices in LPJ-GUESS improve the spatial representation of environmental variables? (2016).

47. *Anna Lundgren:* Development of a method for mapping the highest coastline in Sweden using breaklines extracted from high resolution digital elevation models (2016).

48. *Oluwatomi Esther Adejoro:* Does location also matter? A spatial analysis of social achievements of young South Australians (2016).

49. *Hristo Dobrev Tomov:* Automated temporal NDVI analysis over the Middle East for the period 1982 - 2010 (2016).

50. *Vincent Muller:* Impact of Security Context on Mobile Clinic Activities A GIS Multi Criteria Evaluation based on an MSF Humanitarian Mission in Cameroon (2016).

51. *Gezahagn Negash Seboka:* Spatial Assessment of NDVI as an Indicator of Desertification in Ethiopia using Remote Sensing and GIS (2016).

52. *Holly Buhler:* Evaluation of Interfacility Medical Transport Journey Times in Southeastern British Columbia. (2016).

53. *Lars Ole Grottenberg*: Assessing the ability to share spatial data between emergency management organisations in the High North (2016).

54. *Sean Grant:* The Right Tree in the Right Place: Using GIS to Maximize the Net Benefits from Urban Forests (2016).

55. *Irshad Jamal:* Multi-Criteria GIS Analysis for School Site Selection in Gorno-Badakhshan Autonomous Oblast, Tajikistan (2016).

56. *Fulgencio Sanmartín:* Wisdom-volkano: A novel tool based on open GIS and time-series visualization to analyse and share volcanic data (2016).

57. *Nezha Acil:* Remote sensing-based monitoring of snow cover dynamics and its influence on vegetation growth in the Middle Atlas Mountains (2016).

58. *Julia Hjalmarsson:* A Weighty Issue: Estimation of Fire Size with Geographically Weighted Logistic Regression (2016).

59. *Mathewos Tamiru Amato:* Using multi-criteria evaluation and GIS for chronic food and nutrition insecurity indicators analysis in Ethiopia (2016).

60. *Karim Alaa El Din Mohamed Soliman El Attar:* Bicycling Suitability in Downtown, Cairo, Egypt (2016).

61. *Gilbert Akol Echelai:* Asset Management: Integrating GIS as a Decision Support Tool in Meter Management in National Water and Sewerage Corporation (2016).

62. *Terje Slinning:* Analytic comparison of multibeam echo soundings (2016).

63. *Gréta Hlín Sveinsdóttir:* GIS-based MCDA for decision support: A framework for wind farm siting in Iceland (2017).

64. *Jonas Sjögren:* Consequences of a flood in Kristianstad, Sweden: A GIS-based analysis of impacts on important societal functions (2017).

65. *Nadine Raska:* 3D geologic subsurface modelling within the Mackenzie Plain, Northwest Territories, Canada (2017).

66. *Panagiotis Symeonidis*: Study of spatial and temporal variation of atmospheric optical parameters and their relation with PM 2.5 concentration over Europe using GIS technologies (2017).

67. *Michaela Bobeck:* A GIS-based Multi-Criteria Decision Analysis of Wind Farm Site Suitability in New South Wales, Australia, from a Sustainable Development Perspective (2017).

68. *Raghdaa Eissa*: Developing a GIS Model for the Assessment of Outdoor Recreational Facilities in New Cities Case Study: Tenth of Ramadan City, Egypt (2017).

69. *Zahra Khais Shahid*: Biofuel plantations and isoprene emissions in Svea and Götaland (2017).

70. *Mirza Amir Liaquat Baig*: Using geographical information systems in epidemiology: Mapping and analyzing occurrence of diarrhea in urban - residential area of Islamabad, Pakistan (2017).

71. *Joakim Jörwall*: Quantitative model of Present and Future well-being in the EU-28: A spatial Multi-Criteria Evaluation of socioeconomic and climatic comfort factors (2017).

72. *Elin Haettner*: Energy Poverty in the Dublin Region: Modelling Geographies of Risk (2017).

73. *Harry Eriksson*: Geochemistry of stream plants and its statistical relations to soil- and bedrock geology, slope directions and till geochemistry. A GIS-analysis of small catchments in northern Sweden (2017).

74. *Daniel Gardevärn:* PPGIS and Public meetings – An evaluation of public participation methods for urban planning (2017).

75. *Kim Friberg:* Sensitivity Analysis and Calibration of Multi Energy Balance Land Surface Model Parameters (2017).

76. *Viktor Svanerud:* Taking the bus to the park? A study of accessibility to green areas in Gothenburg through different modes of transport (2017).

77. *Lisa-Gaye Greene*: Deadly Designs: The Impact of Road Design on Road Crash Patterns along Jamaica's North Coast Highway (2017).

78. *Katarina Jemec Parker*: Spatial and temporal analysis of fecal indicator bacteria concentrations in beach water in San Diego, California (2017).

79. *Angela Kabiru*: An Exploratory Study of Middle Stone Age and Later Stone Age Site Locations in Kenya's Central Rift Valley Using Landscape Analysis: A GIS Approach (2017).

80. *Kristean Björkmann*: Subjective Well-Being and Environment: A GIS-Based Analysis (2018).

81. *Williams Erhunmonmen Ojo*: Measuring spatial accessibility to healthcare for people living with HIV-AIDS in southern Nigeria (2018).

82. *Daniel Assefa*: Developing Data Extraction and Dynamic Data Visualization (Styling) Modules for Web GIS Risk Assessment System (WGRAS). (2018).

83. *Adela Nistora*: Inundation scenarios in a changing climate: assessing potential impacts of sea-level rise on the coast of South-East England (2018).

84. *Marc Seliger*: Thirsty landscapes - Investigating growing irrigation water consumption and potential conservation measures within Utah's largest master-planned community: Daybreak (2018).

85. *Luka Jovičić*: Spatial Data Harmonisation in Regional Context in Accordance with INSPIRE Implementing Rules (2018).

86. *Christina Kourdounouli*: Analysis of Urban Ecosystem Condition Indicators for the Large Urban Zones and City Cores in EU (2018).

87. *Jeremy Azzopardi*: Effect of distance measures and feature representations on distance-based accessibility measures (2018).

88. *Patrick Kabatha*: An open source web GIS tool for analysis and visualization of elephant GPS telemetry data, alongside environmental and anthropogenic variables (2018).

89. *Richard Alphonce Giliba*: Effects of Climate Change on Potential Geographical Distribution of Prunus africana (African cherry) in the Eastern Arc Mountain Forests of Tanzania (2018).

90. *Eiður Kristinn Eiðsson*: Transformation and linking of authoritative multi-scale geodata for the Semantic Web: A case study of Swedish national building data sets (2018).

91. *Niamh Harty*: HOP!: a PGIS and citizen science approach to monitoring the condition of upland paths (2018).

92. *José Estuardo Jara Alvear*: Solar photovoltaic potential to complement hydropower in Ecuador: A GIS-based framework of analysis (2018).

93. *Brendan O'Neill*: Multicriteria Site Suitability for Algal Biofuel Production Facilities (2018).

94. *Roman Spataru*: Spatial-temporal GIS analysis in public health – a case study of polio disease (2018).

95. *Alicja Miodońska*: Assessing evolution of ice caps in Suðurland, Iceland, in years 1986 - 2014, using multispectral satellite imagery (2019).

96. *Dennis Lindell Schettini*: A Spatial Analysis of Homicide Crime's Distribution and Association with Deprivation in Stockholm Between 2010-2017 (2019).

97. *Damiano Vesentini*: The Po Delta Biosphere Reserve: Management challenges and priorities deriving from anthropogenic pressure and sea level rise (2019).

98. *Emilie Arnesten*: Impacts of future sea level rise and high water on roads, railways and environmental objects: a GIS analysis of the potential effects of increasing sea levels and highest projected high water in Scania, Sweden (2019).

99. *Syed Muhammad Amir Raza*: Comparison of geospatial support in RDF stores: Evaluation for ICOS Carbon Portal metadata (2019).

100. *Hemin Tofiq*: Investigating the accuracy of Digital Elevation Models from UAV images in areas with low contrast: A sandy beach as a case study (2019).

101. *Evangelos Vafeiadis*: Exploring the distribution of accessibility by public transport using spatial analysis. A case study for retail concentrations and public hospitals in Athens (2019).

102. *Milan Sekulic*: Multi-Criteria GIS modelling for optimal alignment of roadway by-passes in the Tlokweng Planning Area, Botswana (2019).

103. *Ingrid Piirisaar*: A multi-criteria GIS analysis for siting of utility-scale photovoltaic solar plants in county Kilkenny, Ireland (2019).

104. *Nigel Fox*: Plant phenology and climate change: possible effect on the onset of various wild plant species' first flowering day in the UK (2019).

105. *Gunnar Hesch*: Linking conflict events and cropland development in Afghanistan, 2001 to 2011, using MODIS land cover data and Uppsala Conflict Data Programme (2019).

106. *Elijah Njoku*: Analysis of spatial-temporal pattern of Land Surface Temperature (LST) due to NDVI and elevation in Ilorin, Nigeria (2019).

107. *Katalin Bunyevácz*: Development of a GIS methodology to evaluate informal urban green areas for inclusion in a community governance program (2019).

108. *Paul dos Santos*: Automating synthetic trip data generation for an agent-based simulation of urban mobility (2019).

109. *Robert O' Dwyer*: Land cover changes in Southern Sweden from the mid-Holocene to present day: Insights for ecosystem service assessments (2019).

110. *Daniel Klingmyr*: Global scale patterns and trends in tropospheric NO2 concentrations (2019).

111. *Marwa Farouk Elkabbany*: Sea Level Rise Vulnerability Assessment for Abu Dhabi, United Arab Emirates (2019).

112. *Jip Jan van Zoonen*: Aspects of Error Quantification and Evaluation in Digital Elevation Models for Glacier Surfaces (2020).

113. *Georgios Efthymiou*: The use of bicycles in a mid-sized city – benefits and obstacles identified using a questionnaire and GIS (2020).

114. *Haruna Olayiwola Jimoh*: Assessment of Urban Sprawl in MOWE/IBAFO Axis of Ogun State using GIS Capabilities (2020).

115. *Nikolaos Barmpas Zachariadis*: Development of an iOS, Augmented Reality for disaster management (2020).

116. *Ida Storm*: ICOS Atmospheric Stations: Spatial Characterization of CO2 Footprint Areas and Evaluating the Uncertainties of Modelled CO2 Concentrations (2020).

117. *Alon Zuta*: Evaluation of water stress mapping methods in vineyards using airborne thermal imaging (2020).

118. *Marcus Eriksson*: Evaluating structural landscape development in the municipality Upplands-Bro, using landscape metrics indices (2020).

119. *Ane Rahbek Vierø*: Connectivity for Cyclists? A Network Analysis of Copenhagen's Bike Lanes (2020).

120. *Cecilia Baggini*: Changes in habitat suitability for three declining Anatidae species in saltmarshes on the Mersey estuary, North-West England (2020).

121. *Bakrad Balabanian*: Transportation and Its Effect on Student Performance (2020).

122. *Ali Al Farid*: Knowledge and Data Driven Approaches for Hydrocarbon Microseepage Characterizations: An Application of Satellite Remote Sensing (2020).

123. *Bartlomiej Kolodziejczyk*: Distribution Modelling of Gene Drive-Modified Mosquitoes and Their Effects on Wild Populations (2020).

124. *Alexis Cazorla*: Decreasing organic nitrogen concentrations in European water bodies - links to organic carbon trends and land cover (2020).

125. *Kharid Mwakoba*: Remote sensing analysis of land cover/use conditions of community-based wildlife conservation areas in Tanzania (2021).

126. *Chinatsu Endo*: Remote Sensing Based Pre-Season Yellow Rust Early Warning in Oromia, Ethiopia (2021).

127. *Berit Mohr*: Using remote sensing and land abandonment as a proxy for long-term human out-migration. A Case Study: Al-Hassakeh Governorate, Syria (2021).

128. *Kanchana Nirmali Bandaranayake*: Considering future precipitation in delineation locations for water storage systems - Case study Sri Lanka (2021).

129. *Emma Bylund*: Dynamics of net primary production and food availability in the aftermath of the 2004 and 2007 desert locust outbreaks in Niger and Yemen (2021).

130. *Shawn Pace*: Urban infrastructure inundation risk from permanent sea-level rise scenarios in London (UK), Bangkok (Thailand) and Mumbai (India): A comparative analysis (2021).

131. *Oskar Evert Johansson*: The hydrodynamic impacts of Estuarine Oyster reefs, and the application of drone technology to this study (2021).

132. *Pritam Kumarsingh*: A Case Study to develop and test GIS/SDSS methods to assess the production capacity of a Cocoa Site in Trinidad and Tobago (2021).

133. *Muhammad Imran Khan*: Property Tax Mapping and Assessment using GIS (2021).

134. *Domna Kanari*: Mining geosocial data from Flickr to explore tourism patterns: The case study of Athens (2021).

135. *Mona Tykesson Klubien*: Livestock-MRSA in Danish pig farms (2021).

136. *Ove Njøten*: Comparing radar satellites. Use of Sentinel-1 leads to an increase in oil spill alerts in Norwegian waters (2021).

137. *Panagiotis Patrinos*: Change of heating fuel consumption patterns produced by the economic crisis in Greece (2021).

138. *Lukasz Langowski*: Assessing the suitability of using Sentinel-1A SAR multi-temporal imagery to detect fallow periods between rice crops (2021).

139. *Jonas Tillman*: Perception accuracy and user acceptance of legend designs for opacity data mapping in GIS (2022).

140. *Gabriela Olekszyk*: ALS (Airborne LIDAR) accuracy: Can potential low data quality of ground points be modelled/detected? Case study of 2016 LIDAR capture over Auckland, New Zealand (2022).

141. *Luke Aspland*: Weights of Evidence Predictive Modelling in Archaeology (2022).

142. *Luís Fareleira Gomes*: The influence of climate, population density, tree species and land cover on fire pattern in mainland Portugal (2022).

143. *Andreas Eriksson*: Mapping Fire Salamander (Salamandra salamandra) Habitat Suitability in Baden-Württemberg with Multi-Temporal Sentinel-1 and Sentinel-2 Imagery (2022).

144. *Lisbet Hougaard Baklid*: Geographical expansion rate of a brown bear population in Fennoscandia and the factors explaining the directional variations (2022).

145. *Victoria Persson*: Mussels in deep water with climate change: Spatial distribution of mussel (Mytilus galloprovincialis) growth offshore in the French Mediterranean with respect to climate change scenario RCP 8.5 Long Term and Integrated Multi-Trophic Aquaculture (IMTA) using Dynamic Energy Budget (DEB) modelling (2022).

146. *Benjamin Bernard Fabien Gérard Borgeais*: Implementing a multi-criteria GIS analysis and predictive modelling to locate Upper Palaeolithic decorated caves in the Périgord noir, France (2022).

147. *Bernat Dorado-Guerrero*: Assessing the impact of post-fire restoration interventions using spectral vegetation indices: A case study in El Bruc, Spain (2022).

148. *Ignatius Gabriel Aloysius Maria Perera*: The Influence of Natural Radon Occurrence on the Severity of the COVID-19 Pandemic in Germany: A Spatial Analysis (2022).

149. *Mark Overton*: An Analysis of Spatially-enabled Mobile Decision Support Systems in a Collaborative Decision-Making Environment (2022).

150. *Viggo Lunde*: Analysing methods for visualizing time-series datasets in open-source web mapping (2022).

151. *Johan Viscarra Hansson*: Distribution Analysis of Impatiens glandulifera in Kronoberg County and a Pest Risk Map for Alvesta Municipality (2022).

152. *Vincenzo Poppiti*: GIS and Tourism: Developing strategies for new touristic flows after the Covid-19 pandemic (2022).

153. *Henrik Hagelin*: Wildfire growth modelling in Sweden - A suitability assessment of available data (2023).

154. *Gabriel Romeo Ferriols Pavico*: Where there is road, there is fire (influence): An exploratory study on the influence of roads in the spatial patterns of Swedish wildfires of 2018 (2023).

155. *Colin Robert Potter*: Using a GIS to enable an economic, land use and energy output comparison between small wind powered turbines and large-scale wind farms: the case of Oslo, Norway (2023).

156. *Krystyna Muszel*: Impact of Sea Surface Temperature and Salinity on Phytoplankton blooms phenology in the North Sea (2023).

157. *Tobias Rydlinge*: Urban tree canopy mapping - an open source deep learning approach (2023).

158. *Albert Wellendorf*: Multi-scale Bark Beetle Predictions Using Machine Learning (2023).

159. *Manolis Papadakis*: Use of Satellite Remote Sensing for Detecting Archaeological Features: An Example from Ancient Corinth, Greece (2023).

160. *Konstantinos Sourlamtas*: Developing a Geographical Information System for a water and sewer network, for monitoring, identification and leak repair - Case study: Municipal Water Company of Naoussa, Greece (2023).

161. *Xiaoming Wang*: Identification of restoration hotspots in landscape-scale green infrastructure planning based on model-predicted connectivity forest (2023).

162. *Sarah Sienaert*: Usability of Sentinel-1 C-band VV and VH SAR data for the detection of flooded oil palm (2023).

163. *Katarina Ekeroot*: Uncovering the spatial relationships between Covid-19 vaccine coverage and local politics in Sweden (2023).

164. *Nikolaos Kouskoulis*: Exploring patterns in risk factors for bark beetle attack during outbreaks triggered by drought stress with harvester data on attacked trees: A case study in Southeastern Sweden (2023).

165. *Jonas Almén*: Geographic polarization and clustering of partisan voting: A local-level analysis of Stockholm Municipality (2023).